HHS Public Access

Author manuscript

Nat Rev Drug Discov. Author manuscript; available in PMC 2019 August 05.

Published in final edited form as:

Nat Rev Drug Discov. 2019 January ; 18(1): 59–82. doi:10.1038/nrd.2018.180.

GPCR drug discovery: integrating solution NMR data with crystal and cryo-EM structures

Ichio Shimada[*,1], **Takumi Ueda**[1], **Yutaka Kofuku**[1], **Matthew T. Eddy**[§,2,3], **Kurt Wüthrich**[*,2,4]

[1]Graduate School of Pharmaceutical Sciences, The University of Tokyo, Hongo, Bunkyo-ku, Tokyo 113-0033, Japan

[2]Department of Integrative Structural and Computational Biology, Skaggs Institute of Chemical Biology, The Scripps Research Institute, 10550 North Torrey Pines Road, La Jolla, CA 92037, USA

[3]Departments of Biological Sciences and Chemistry, Bridge Institute, USC Michelson Center, University of Southern California, 1002 West Childs Way, Los Angeles, CA 90089, USA

[4]Skaggs Institute of Chemical Biology, The Scripps Research Institute, 10550 North Torrey Pines Road, La Jolla, CA 92037, USA

Abstract

The 826 G protein-coupled receptors (GPCRs) in the human proteome regulate key physiological processes, and thus have long been attractive as drug targets. With crystal structure determinations of more than 50 different human GPCRs during the last decade, an initial platform for structure-based rational design has been established for drugs that target GPCRs, which is currently being augmented with cryo-EM structures of higher-order GPCR complexes. Nuclear magnetic resonance (NMR) spectroscopy in solution is one of the key approaches for expanding this platform with dynamic features, which can be accessed at physiological temperature and with minimal modification of the wild-type GPCR covalent structures. Here, we review strategies for the use of advanced biochemistry and NMR techniques with GPCRs, survey projects where crystal or cryo-EM structures have been complemented with NMR investigations, and discuss the impact of this integrative approach on GPCR biology and drug discovery.

More than 30% of all drugs approved by the US Food and Drug Administration target G protein-coupled receptors (GPCRs)[1–3], and these drugs are utilized in a wide range of therapeutic areas, including inflammation and diseases of the central nervous system as well as the cardiovascular, respiratory and gastrointestinal systems[2,4]. Currently more than 300 agents are in clinical trials, of which around 60 target novel GPCRs for which no drug has as yet been approved[2]. The novel GPCR targets also include orphan GPCRs, for which endogenous ligands have not yet been discovered[2]. Overall, the drugs approved so far target only 27% of the human non-olfactory GPCRs[2], indicating that much excitement still lies ahead.

Identifying new GPCR drugs will need additional detailed knowledge of GPCR biology, especially knowledge from structural biology, given the complex structure–function relationships involved in

[*]Corresponding authors: wuthrich@scripps.edu, shimada@iw-nmr.f.u-tokyo.ac.jp.
[§]Present address: Department of Chemistry, University of Florida, Gainesville, Florida 32611, USA

GPCR signaling. Along this line, recent reviews on GPCRs have covered studies with antibodies[5] and nanobodies[6], allosteric modulation[7–10] biased signaling[11–15], methods in GPCR structural biology[16–19], GPCR crystal structures[20–27] and drug development[2,4,28,29], with some reviews addressing specific GPCR families[30,31]. Complementing the substantial number of GPCR crystal structures that have become available in the past decade, as well as the recent demonstrations of the potential for cryo-EM to provide information on higher-order GPCR complexes[32–36], dynamic studies of GPCRs are important for providing new insights into GPCR biology that can assist drug discovery. In this respect, nuclear magnetic resonance (NMR) spectroscopy in solution is a key tool for analysing function-related conformational equilibria in GPCRs as they relate to allosteric coupling, variable efficacies and biased signaling of GPCR ligands, which are of particular interest for their potential as drugs. Furthermore, NMR spectroscopy is also a useful tool for fragment-based lead discovery with GPCR targets.

In this article, we first overview the structural biology of GPCRs based on knowledge from X-ray crystallography, cryo-EM and solution NMR, and then focus on the application of solution NMR to enhance understanding of GPCR biology relevant to drug discovery, as well as in fragment-based lead discovery. Solid-state NMR studies can also be valuable in the study of GPCR and other membrane protein structures, but have been reviewed elsewhere[37–43] and are not covered here.

Structural biology of GPCRs

Human GPCR biology.

GPCRs are one of the largest membrane protein families in eukaryotes. There are 826 GPCRs in the human proteome, which are classified into five main families based on sequence homology and phylogenetic analyses: rhodopsin family (Class A), secretin family (Class B), glutamate family (Class C), frizzled family (Class F), and adhesion family[22,44]. GPCRs function as receptors for various neurotransmitters, hormones, cytokines (chemokines), metabolites, tastants, and odorants. As well as being a key class of drug targets, GPCRs are frequent “off-targets” of drugs that target other proteins, which can result in unanticipated side effects, and mutations of GPCRs have been linked to dozens of monogenic diseases[22,29].

Activated GPCRs induce signal transduction mediated by G proteins, GPCR kinases (GRKs) and arrestins[12,16,22,24,45] (Fig. 1a). Upon G protein activation, the Gα subunit dissociates from the Gβγ subunits and modulates production of second messengers such as cAMP. Gβγ modulates downstream signaling networks, including ion channels and phospholipases. In addition, the activated GPCRs may be phosphorylated by GRKs, and the phosphorylated GPCRs stimulate G protein-independent signal transduction mediated by arrestins (Fig. 1a), such as receptor internalization and activation of kinase signaling networks.

Different GPCR ligands can modulate signaling through G protein and arrestin pathways differently, and the ligands that preferentially modulate one of the signaling pathways are referred to as ‘biased ligands’[11–15,45–49] (Fig. 1b). Differences in biased signaling critically affect the therapeutic properties of GPCR ligands. Drugs can thus produce side effects mediated through the activation of “unwanted” signaling pathways by the targeted GPCR. It

is of keen interest to minimize such side effects by designing biased ligands that selectively activate the signaling pathway required to produce the desired therapeutic response[11,12,50,51]. For example, G protein-biased agonists of the μ-opioid receptor (MOR) increase the analgesia and reduce the on-target adverse effects compared with morphine[52–57], and several novel biased ligands are under evaluation in clinical trials[12] (Fig. 1c). This work is of great socio-economic interest owing to the crisis caused by the misuse of prescription opiates in the United States[58]. In addition to the bias between the G protein and arrestin pathways, many other types of bias have been proposed, including those between different G protein subtypes[59].

GPCRs exhibit variable basal activities in the absence of bound ligands, and each ligand for a given GPCR has a characteristic level of ability to activate or deactivate its target, which is commonly referred to as its “efficacy”. According to their efficacies, GPCR ligands are classified as full agonists, partial agonists, antagonists and inverse agonists (Fig. 1d)[22,60]. These differences in the efficacies affect the therapeutic properties of the GPCR ligands, and partial agonists can offer clinical advantages over full agonists and antagonists (Fig. 1e)[11,61–64].

Most descriptions of biased agonism were initially based on studies using recombinant cell systems[50]. Although consistent and robust responses of different signaling pathways can thus be obtained [50], many factors can confound the interpretation of these assays, including off-target effects, cell backgrounds, receptor and effector expression levels, and the kinetic properties of agonists[11,50,65]. Thus, the integration of studies using recombinant cell systems with structural biology, detecting direct effects on the receptor conformation, is important in studying biased agonism.

X-ray crystal and cryo-EM structures of human GPCRs.

Since the first crystal structure of bovine rhodopsin published in 2000[66] and the first crystal structure of a human GPCR, β_2AR, published in 2007[67,68], the number of GPCR crystal structures has rapidly increased, so that structures of more than 50 different GPCRs and over 250 of their complexes with different ligands are presently available in the Protein Data Bank, as documented in the GPCRdb[69] (Fig. 2). This includes structures of Class A, Class B, Class C, and Class F receptors[69]. Cryo-EM structures of GPCRs in complexes with partner proteins are also appearing at an increasingly rapid pace. Examples include tertiary complexes of receptors with G proteins and agonists of the glucagon-like peptide-1 receptor (GLP-1R)[35], the calcitonin receptor[36], the A_1 adenosine receptor[70], the μ-opioid receptor[71], the serotonin $5HT_{1B}$ receptor[33], and rhodopsin[34].

Crystal structures have revealed the GPCR three-dimensional architectures, locations of bound ligands and atomic details of receptor–ligand interactions. All Class A GPCRs share a structural topology characterized by seven transmembrane helices (TMI to TMVII) linked by three intracellular loops (ICL) and three extracellular loops (ECL). A canonical “orthosteric” ligand binding pocket facing the extracellular surface is formed by residues of transmembrane helices and extracellular loops (Fig. 2)[22,72]. Crystal structures have also identified ligand binding sites in transmembrane regions outside of the orthosteric pocket of Class A[73] and Class B[74] receptors, which relate to allosteric modulation of effects from

orthosteric ligand binding (Fig. 2). In GPCR crystal structures determined at resolutions of 2.5 Å or higher, small molecules and ions have been observed, including bound sodium[75,76], networks of crystallographic water molecules[75], lipids and cholesterol[77], providing a structural basis for rationalizing the regulation of GPCRs by allosteric modulators. Knowledge about mechanisms underlying allosteric modulators can in turn provide novel insights into the signal transduction through GPCRs. Exogenous allosteric modulators may be useful for the development of GPCR subtype-specific drugs, where different subtypes may have nearly identical orthosteric sites[78].

The crystal structures of the β_2-adrenergic receptor (β_2AR) indicated the following structural mechanism for Class A GPCR activation[78–81] (Fig. 3a). Full agonists induce a rearrangement of the interactions between TM helices in the central part of the GPCR structure, i.e., an inward shift of TMV at P211$^{5.50}$, an axial shift of TMIII at I121$^{3.40}$, and an outward shift of TMVI starting at F282$^{6.44}$ (the four-digit superscripts indicate the Ballesteros-Weinstein nomenclature[82] for amino acid residues in GPCRs, where the first number indicates the helix in which the residue is located). These three residues are referred to as the P/I/F motif. The rearrangement of the TM helices induces a large outward movement of the cytoplasmic half of TMVI, and thus increases the distance between TMIII and TMVI in the cytoplasmic region and disrupts a salt bridge in an ionic lock, which accompanies the repositioning of the sidechain of Y326$^{7.53}$ in a second highly conserved motif consisting of residues NPxxY. The residues that exhibit conformational changes upon activation of β_2AR are highly conserved among the Class A GPCRs[81,83,84], and when comparing antagonist-bound states and ternary complexes with agonists and G protein-mimetics, similar conformational differences were observed for other Class A GPCRs. Similar conformational changes upon activation (Fig. 3a) thus seem to be characteristic among the Class A GPCRs.

In a crystal structure of the ternary complex of β_2AR with a full agonist and a G protein[85], a cytoplasmic cavity is formed by the outward shift of the cytoplasmic half of TM V and TMVI and the distortion of TMVII, when compared with their conformations in the inverse agonist-bound form[68]; the C-terminal helix of the G protein is then inserted into the cytoplasmic cavity. Similar cytoplasmic cavity formation was observed for the crystal structures of other GPCRs in tertiary complexes with a full agonist and a G protein mimetic[86] as well as for cryo-EM structures of GPCRs in tertiary complexes with an agonist and G protein[33,34,70,71].

GPCR crystal structures have been extensively utilized for structure-based drug design, and there are more than 30 reports on *in silico* screening of GPCR ligands, some of which resulted in identification of GPCR ligands with novel chemical scaffolds[22,87]. However, information on GPCR features that are of special interest to in drug discovery, such as basal activity, biased signaling, partial agonism, and allosteric modulation by ions and small molecules can only be partially derived from crystallography data. These limitations arise in large part from the well-established practice of making modifications to the wild-type GPCR covalent structure to facilitate crystallization, such as truncation of flexible domains and chain ends, introduction of soluble fusion proteins into the loops or at the receptor N-terminus[88,89], and systematic replacement of endogenous amino acids to increase the

thermostability[90–92]. Alternatively, crystallization has also been facilitated by the formation of stable non-covalent complexes with a partner protein, such as an engineered G protein[93], antibody[94] or nanobody[6,81], but this can also affect functionally relevant conformational equilibria.

An illustration of the limitations is provided by the β_1 adrenergic receptor (β_1AR), which was thermostabilized by modifications that also trap the receptor in an inactive state. The crystal structures then showed nearly identical conformations for complexes with antagonists, a partial agonist, a full agonist, and a biased agonist[92,95].

GPCR crystallography also depends on the selection of the orthosterically bound ligand. All small-molecule ligands used so far appear to have similar chemical properties and high binding affinity (Ki ≤10 nM)[96], thus probably providing information on only a fraction of the drug scaffolds that can potentially be recognized by GPCRs. Crystal structure determination is particularly challenging for GPCRs that bind endogenous or synthetic peptides, so that only a few crystal structures have so far been determined for GPCRs in complex with peptides[23]; these include endothelin[97], neurotensin[98], and the neuropeptide Y_1 receptor[99]. As peptide therapeutics are promising[2], especially for Class B GPCRs, other techniques such as NMR may be valuable in providing more comprehensive structural information on GPCR-peptide drug systems.

In summary, the success of GPCR crystallography has also revealed the need to complement crystal structures with data collected with different techniques in milieus that are closer to physiological conditions than the crystalline state and liquid nitrogen temperature, and solution NMR is particularly promising in this respect.

NMR data and GPCR functions.

NMR methods provide information about dynamics of proteins over a wide range of frequencies in aqueous solutions at near-physiological temperature[100–102]. NMR studies thus revealed that global and local conformational fluctuations of protein structures are tightly related to their functions, such as enzymatic activities[103,104] or molecular recognition[105], especially also in membrane proteins[106–109]. Although NMR studies of GPCRs are challenging, observations of the NMR signals of various GPCRs have been accomplished through recent methodological advances, including ultra-high-field NMR instruments, improved cryogenic probes, transverse relaxation-optimized spectroscopy (TROSY)[110,111], and refined methods for labeling with stable isotopes and other NMR probes (Box 1).

NMR studies, along with various other spectroscopic studies, have revealed that GPCRs exist in function-related equilibria between multiple locally different conformations that are simultaneously populated. These function-related equilibria are typically abolished by the modifications used for crystallography studies described above. NMR studies thus provide information that is complementary to data from X-ray crystallography and cryo-EM studies, which should be considered in functional interpretations of GPCR crystal structures. NMR can also be used for serial analyses of the conformations of GPCRs bound to various ligands with different efficacies and extent of biased signaling[112–115], whereas the determination of

the crystal structures in a wider range of ligand-bound states is not straightforward for GPCRs[22]. Table 1 summarizes recent NMR studies of conformational equilibria in GPCRs that relate to partial agonism and biased signaling[112–131], and which aim at facilitating the design of new compounds that can modulate GPCR signaling.

In addition to observing GPCRs and their interactions with drugs and partner proteins, NMR has been used to directly observe GPCR ligands in both their unbound and receptor-bound conformations. This enables the determination of structures of GPCR ligands and measurement of their conformational dynamics while bound to the receptor and, in principle, their drug pharmacokinetics. Some examples from a very large array of literature data on this topic include the determination of the structure of the agonist dynorphin bound to the κ-opioid receptor[132], the cytokine interleukine-8 and its interactions with the chemokine receptor CXCR1[133,134], lipids of the free fatty acid receptor[135], and peptide agonists of the bradykinin receptors[136]. Importantly, NMR can be used to monitor the relatively weak interactions of low-molecular-mass compounds with GPCRs, and therefore can support fragment-based lead discovery approaches. Finally, NMR has been used to study the structure and dynamics of GPCR partner proteins, including G proteins and arrestins, and their interactions with GPCRs and nucleotides[137–139]. Thus, in addition to information from NMR observation of GPCRs, NMR can provide a comprehensive view of a wide range of molecules that interact with GPCRs and modulate GPCR signaling.

NMR studies of human GPCRs

NMR studies on the dynamics of GPCRs related to their functions have so far typically been performed in the following manner. First, labeled GPCRs are prepared using fluorine and/or stable-isotope labeling methods (Box 1) and reconstituted in detergent micelles or lipid nanodiscs (Box 2). Second, resolved NMR signals are observed and assigned, and structural and dynamics information is obtained from the resonances. For example, the ^{13}C chemical shifts of side-chain methyl signals probe the side-chain conformation[140,141], the ^{1}H and ^{19}F chemical shifts of side-chain $^{13}CH_3$ and CF_3 groups probe their local environments, including the ring current effects from neighboring aromatic residues[113,142,143], and the solvent accessibility of the observed atoms can be assessed by the addition of paramagnetic probes to the solvent[112,144]. Exchange rates and species populations in conformational equilibria can be determined with line-shape analysis[145], CPMG[122], saturation transfer[119,120,122] and exchange spectroscopy[120], including perturbation of an equilibrium by changing the temperature. The functional relevance of the observed conformational changes can then be explored by investigations of the relationships between the NMR spectra and the signaling activities of the GPCRs.

In the following sections, results obtained by using these approaches with different individual GPCRs are described, with most examples from GPCRs in Class A, which is the largest phylogenetic class of GPCRs[79]. Among almost 700 Class A GPCRs, 296 are non-olfactory GPCRs which function as receptors of various hormones and neurotransmitters, and are the most commonly exploited GPCRs for pharmacological interventions[22]. NMR studies of Class A GPCRs have provided insights into the mechanisms enabling partial agonism and biased signaling, with β_2AR as the representative of Class A GPCRs with the

most extensive set of experimental data. Exploratory NMR measurements with other Class A GPCRs have clearly indicated that all the information gathered for β_2AR is not readily applicable for other GPCRs, and increasing interest has recently been focused on structural and functional studies of other Class A GPCRs.

β_2-adrenergic receptor.

The conformational dynamics of β_2AR, a Class A GPCR stimulated by adrenaline and various bronchodilators, has been extensively studied by multiple groups (Table 1). NMR signals have been observed for CF_3 groups of 2,2,2-trifluoroethanethiol (TET)[112,120], 3-bromo-1,1,1-trifluoroacetone (BTFA)[117,119], and 2-bromo-4-trifluoromethyl-acetanilide (BTFMA)[122,146], which were covalently linked to cysteine residues near to the cytoplasmic surface. Additional studies were based on observation of $^{13}CH_3$ signals of reductively ^{13}C-methylated lysine residues near the extracellular surface[116] and for $^{13}CH_3$-labeled methionine residues[113,118,121], which are widely distributed in the transmembrane region. Overall, NMR data are now available from observation of probes in strategic locations distributed over the entire three-dimensional molecular structure. In addition, other methods, including fluorescence spectroscopy[147–154], electron paramagnetic resonance (EPR)[122], chemical labeling[155,156], and hydrogen–deuterium exchange[157], have been utilized for studying the conformation of β_2AR. These data have enabled examinations of the global conformational dynamics that determines the efficacies and biased signaling of β_2AR.

Conformational equilibria related to variations in ligand efficacy have been observed in various regions of β_2AR, using NMR probes located primarily in positions where large differences were observed between crystal structures of inactive and active-like states[68,85]. With CF_3 probes at C265$^{6.27}$ and C327$^{7.54}$ near the cytoplasmic tips of TMVI and TMVII, respectively, equilibria between inactive and active-like conformations were observed, with exchange rates slower than 10 s^{-1}[112,120], and the population of the active-like state correlated with the ligand efficacy[112] (Fig. 4). The exchange rates observed using a single-molecule fluorescence probe at C265$^{6.27}$ were similar to those observed using the CF_3 probe[152].

Additionally, faster intramolecular rate processes were discovered by observation of the M82 side chain, which reflects the conformation of the P/I/F motif in the central transmembrane region[113]. Equilibria among two conformations containing the inactive P/I/F motif, $PIFoff_1$ and $PIFoff_2$, and one conformation with the active P/I/F motif, PIFon, were observed (Fig. 3), and the population of the latter correlated with different ligand efficacies[113]. Remarkably, the exchange rates seen for the P/I/F motif were larger than those observed for the CF_3 probe at C265$^{6.27}$ i.e. ~2,000 s^{-1}. This exchange rate is in closer agreement with k_{ex} >100 s^{-1} observed using single-molecule spectroscopy with FRET probes at the positions N148C$^{4.40}$ and L266C$^{6.28}$. FRET is sensitive to variations of the TMIV–TMVI distance in the interior region, which thus appears to also reflect the conformation of the P/I/F motif. In the case of M215$^{5.54}$, for which the chemical shifts of the peripheral $^{13}CH_3$ group reflect both the activation state of the P/I/F motif and the crystallographically observed conformational changes near the intracellular surface[113], the NMR signals are affected by both of the aforementioned equilibria.

In order to integrate the NMR data with information obtained from other techniques and thus to generate a global view of the structure and conformational dynamics of β_2AR, simulations of the resonances from M82$^{2.53}$, M215$^{5.54}$, and the CF_3 probe at C265$^{6.27}$ were performed. A model that was found to be in agreement with the NMR experiments and the ligand efficacies is depicted in Fig. 3b, where the exchange rates of the P/I/F motif activation are different from those of the conformational exchange near the intracellular surface, as manifested by the ^{19}F probe at C265$^{6.27}$. CPMG experiments with another CF_3 probe, 2-bromo-4-trifluoromethyl-acetanilide, at C265 of β_2AR in the apo and inverse agonist-bound states indicated that C265 underwent conformational rate processes with exchange rates > 1,000 s^{-1} [122,146], suggesting that in the inactive state the cytoplasmic surface region of β_2AR is characterized as a manifold of rapidly exchanging substates.

NMR studies of β_2AR provided a structural basis for biased signaling of GPCRs[112]. Carvedilol and isoetharine share similar chemical structures with the inverse agonist carazolol and the full agonist isoproterenol, respectively, and have been classified as β-arrestin–biased ligands of β-adrenergic receptors[158,159]. Arrestin signaling through β_2AR promotes cardiomyocyte survival, and the arrestin-biased β_2AR ligands represent a potentially useful therapeutic approach[160]. Liu et al. observed the resonances of ^{19}F labels introduced at C265$^{6.27}$ and C327$^{7.54}$, which are at the cytoplasmic ends of TMVI and TMVII of β_2AR, respectively, and demonstrated that β-arrestin-biased ligands predominantly impacted the conformation of C327$^{7.54}$[112] (Fig. 4, a and b). These results suggested that β-arrestin-biased ligands of β_2AR induce conformational changes of TMIII and TMVII, where the populations of inactive and active-like states seen in this location are not paralleled by those seen at C265$^{6.27}$ for TMV and TMVI (Fig. 4c).

Experiments with β-adrenergic receptors have also provided useful lessons for improving the technologies for structural studies of GPCRs. NMR was used to study the effects of the insertion of the fusion protein utilized in crystallographic studies of β_2AR[16] on the function-related conformational equilibria[123]. To this end, the ^{19}F-NMR signals of CF_3 groups introduced at the cytoplasmic ends of TMVI and TMVII were compared for β_2AR with and without T4 lysozyme fused into the ICL3. The fusion of T4 lysozyme into the ICL3 was thus found to block the conformational equilibrium seen at the cytoplasmic tip of TMVI in the active-like state, independent of the ligand bound to β_2AR[123] (Fig. 5a). In addition, in the apo and norepinephrine-bound states, the fusion of T4 lysozyme induced a long-range effect *via* the orthosteric cavity on the conformational equilibrium at the cytoplasmic tip of TMVII (Fig. 5a)[123]. The observation at C265 is in apparent contrast with data from earlier fluorescence experiments with β_2AR-T4L[67], which measured the overall effect of the fusion protein on labels in both positions 265 and 327. In contrast, by individually labeling C265 and C327 in the ^{19}F-NMR study, the separate response at each of the cytoplasmic ends of helices VI and VII could be measured. The NMR results now provide a rationale for the fact that the fluorescence experiments, which were designed before the crystal structure had been known, did not reveal the status of TM VI, because the changes in the fluorescence measurements between agonist and antagonist complexes were dominated by the probe at 327[53]. The results obtained by measurements in solution emphasize that effects of ICL3 fusions and/or thermostabilizing mutations on the conformational equilibria in GPCRs

should be duly considered in functional interpretations of GPCR crystal structures obtained with such protein modifications.

A thermostabilized variant of the β_1-adrenergic receptor (β_1AR), which has 56% sequence identity to β_2AR, was prepared with ^{15}N-labeling of its 28 valines. The [^{15}N,^{1}H]-TROSY correlation NMR spectra (Fig. 5b) contain more than 20 signals, of which a large portion were assigned. Corresponding signals of the antagonist and agonist complexes have closely similar chemical shifts (Fig. 5b), which reflects the previously mentioned fact that the thermostabilization used locks the receptor in the inactive conformation, as confirmed by x-ray crystallography[92]. Nonetheless, NMR spectroscopy revealed subtle differences in line shapes and chemical shifts (Fig. 5b), which were used to obtain novel insights. For example, chemical shift changes upon formation of a ternary complex with the G protein-mimicking nanobody Nb80 were reported for valines located throughout the receptor, representing "reverse" allosteric effects near the extracellular surface from complex formation with the nanobody at the intracellular signaling surface[99]. Allosteric effects of β_1AR complex formation with G protein-mimicking nanobodies were also observed with the use of ^{13}C-methyl-methionine labels[115].

Comparative NMR studies of a β_2AR complex with a partial agonist in nanodiscs and in DDM micelles revealed that the exchange rates between the conformations with inactive and active P/I/F motifs are lower in nanodiscs than in the detergent micelles (Box 2), and that the population of the conformation with an active P/I/F motif of β_2AR is higher in nanodiscs than in DDM micelles (Fig. 5c)[121]. NMR analyses of other membrane proteins embedded in nanodiscs also showed modulation of the conformational equilibria and the functions of membrane proteins by the lipid bilayer environment[108,161]. The maximum cAMP response, calculated using the populations of the conformations with the active P/I/F motif of β_2AR in nanodiscs, correlated better with the experimental values than those calculated for β_2AR in DDM micelles[121] (Fig. 5d). These NMR investigations of GPCRs, and work with other membrane proteins, indicate that data on membrane proteins in detergent micelles need to be carefully evaluated, since different values for relative populations of the different conformational states and the exchange rates between them were measured in the lipid bilayer environment of nanodiscs.

μ-opioid receptor (MOR).

This Class A GPCR is stimulated by various opioid drugs, including morphine. Studies have indicated that MOR signaling through G_i (the inhibitory G protein for adenylyl cyclase) has a key role in the desired analgesic properties of morphine, whereas signaling through β-arrestin is associated with adverse side effects such as respiratory depression[162,163]. This knowledge has led to efforts to identify biased MOR ligands that show enhanced G_i signaling and reduced β-arrestin signaling compared with morphine, including oliceridine (TRV130)[164], PZM21[57] and SR17018[55,56], which result in increased analgesia with reduced on-target adverse effects[52,53,57]. Further understanding of the mechanisms underlying biased MOR signaling are therefore of high interest for the development of much-needed novel analgesics.

Crystal structures of MOR have been solved in various forms, including those bound to inverse agonists and to a full agonist with a G protein-mimicking nanobody[165,166]. Activation-induced conformational changes of the structural motifs that are widely conserved among Class A GPCRs, including the cytoplasmic cavity formation, were also observed for the MOR structures. These crystal structures were complemented in important ways by NMR studies. Sounier et al. used NMR signals originating from $^{13}CH_3$ probes attached to the solvent-accessible lysines of MOR in the apo state, an agonist-bound state, and the ternary complex with an agonist and a G protein-mimicking nanobody[128]. Okude et al. observed the NMR signals of M163$^{3.46}$, M245$^{5.49}$ M257$^{5.61}$ and M283$^{6.36}$ of MOR, which are sensitive to conformational changes of TMIII, V, VI, and VII, in the balanced and biased ligand-bound states[129]. The chemical shifts of these residues correlated well with the bias factors, which are the ratios of the β-arrestin signaling efficacies to the G protein signaling efficacies in each state (Fig. 6a). These results, along with temperature-dependent shifts of these resonances, suggested that the intracellular cavity of MOR exists in an equilibrium between a closed and multiple open conformations, with coupled rearrangements of the transmembrane helices III, V, VI and VII, and that the relative populations of the open conformations determine the G protein- and arrestin-mediated signaling levels in different ligand-bound states (Fig. 6b).

A_{2A} adenosine receptor.

A_{2A}AR plays myriad roles in human health, including regulating myocardial blood flow, and it is heavily expressed in the central nervous system, where it is involved with dopamine and glutamine release[167,168]. A_{2A}AR has recently also become a promising target for developing cancer immunotherapies[169–173]. Similar to β_2AR, A_{2A}AR is structurally well characterized. Crystal structures are available of antagonist complexes[90,174], agonist complexes[175,176], and a ternary complex with an agonist and a “mini” G protein[177]. For NMR spectroscopy it is of interest that A_{2A}AR has been expressed in multiple cell types, including *Pichia pastoris*, insect cells, and mammalian cells, permitting many options for stable-isotope labeling (Box 1).

^{19}F-NMR has been used to study A_{2A}AR by post-translational chemical modification of non-endogenous cysteines introduced at positions near the intracellular surface, which were labeled with ^{19}F-BTFMA[125], or *via* in-membrane chemical modification with TET[178,179], and then studied in detergent micelles. One-dimensional ^{19}F-NMR spectra were measured for A_{2A}AR complexes with ligands of different efficacies. Efficacy-dependent changes of the relative populations of different conformational states were observed[125,179,] which were also shown to respond to variable salt concentrations[131].

[u-^{15}N, ~70% ^{2}H]-human A_{2A}AR was expressed in *Pichia pastoris*, and single-amino acid replacements were used for the assignment of all six tryptophan indole ^{15}N–^{1}H signals and eight glycine backbone ^{15}N-^{1}H signals distributed on the extracellular and intracellular surfaces (Fig 7a)[127]. The distribution of NMR probes (Fig. 7b) permitted a global view of the response of A_{2A}AR structure and dynamics to variable efficacy of bound drugs. Effects of the inactivation of an allosteric center by replacement of residue Asp52$^{2.50}$ with Asn resulted in local changes of the orientation of the toggle switch Trp246$^{6.48}$ relative to the

P/I/F activation motif (Fig. 7,c and d), which are directly correlated with both a change of conformational dynamics at the intracellular surface and loss of G protein signaling[127] (Fig. 7e).

[^{1}H,^{13}C-Ile, u-^{2}H]-A_{2A}AR was expressed in *Pichia pastoris* for methyl TROSY NMR experiments, where residues I92$^{3.40}$ and I292$^{8.47}$ were assigned by amino acid replacement[126]. NMR experiments for A_{2A}AR complexes with ligands of different efficacies indicated that inverse agonists suppressed high-frequency motions on the intracellular signaling surface, and large conformational changes were observed depending on the sodium concentration in the A_{2A}AR solutions[126].

A_{2A}AR has an exceptionally long C-terminal polypeptide “tail” when compared with Class A GPCRs at large, i.e. 122 residues rather than 30 to 40 residues. In crystallization constructs, the A_{2A}AR amino acid sequence was truncated at position 316 in order to facilitate crystallization. NMR studies of the isolated C-terminal polypeptide showed that it is intrinsically disordered[180,181], and additional biophysical data suggested that this intrinsic flexibility is important for complex formation with various partner proteins, including calmodulin[180]. Intrinsically disordered polypeptide segments in GPCRs have been shown to be subject to posttranslational modifications and thought to be critical for interactions with G proteins and other partner proteins[182]. NMR is especially well suited for studying intrinsically disordered polypeptides[183,184].

Class B GPCRs.

Class B GPCRs are composed of a 100- to 150-residue N-terminal extracellular domain (NTD or ECD) and a canonical transmembrane domain with seven transmembrane α-helices. This class comprises 15 receptors, which all bind polypeptide hormones[30,31]. Class B GPCRs are involved in key physiological processes and associated diseases, including diabetes, osteoporosis, cancer, neurodegeneration, cardiovascular disease, migraine and psychiatric disorders[31] and so are attractive drug targets[185]. Examples include numerous glucagon-like peptide 1 receptor (GLP1R) agonists that are in use for the treatment of diabetes, and the peptides tesamorelin, a growth hormone-releasing hormone receptor (GHRHR) agonist, and teduglutide, a glucagon-like peptide 2 receptor (GLP2R) agonist[4,186]. However, no small-molecule agonist drugs directed at Class B receptors have so far been identified, and thus new structural information about Class B GPCRs is expected to open exciting new perspectives[4]. For NMR applications it is of interest that various Class B GPCRs have been reported to exhibit biased signaling and allosteric modulation, and there is accumulating evidence for the importance of these features for the development of drugs that target Class B GPCRs[30]. Differences to Class A GPCRs arise because the residues that exhibit the largest conformational changes upon activation in Class A GPCRs, such as the P/I/F, NPxxY, and D(E)RY motifs[60], are not conserved in Class B GPCRs[31], and furthermore the extracellular N-terminal domain of Class B GPCRs may also be directly involved in the regulation of signaling. Overall, the extensive knowledge on Class A GPCR structures is thus not directly applicable to Class B GPCRs.

Class B GPCRs offer new possibilities for applying NMR to study mechanisms of ligand recognition and intracellular signaling. Most endogenous Class B GPCR ligands are

polypeptides, which can be labeled with stable isotopes[187] to study their detailed atomic interactions with receptors by NMR. The possibility also arises to use NMR in parallel with intein chemistry to selectively label different segments of the GPCR sequence with ^{2}H, ^{15}N and/or ^{13}C. Intein chemistry has been applied to study a C-terminal polypeptide segment of β_2AR[124], and studies of selectively labeled Class B receptor extracellular domains within the full-length receptor would be an obvious extension of this work. NMR can thus provide information by observation of either the endogenous ligand, the GPCR, intracellular partner proteins, or by combinations thereof, since all these components can be individually labeled with NMR-observable probes that provide direct experimental access to ligand and partner protein binding mechanisms that underlie the physiological signaling by Class B GPCRs.

NMR in GPCR drug discovery

The above sections summarize how NMR studies on GPCRs have complemented structural understanding from other biophysical techniques and highlighted opportunities for drug discovery. Here, we discuss the two main ways in which NMR studies can be used in pursuing such opportunities: applications in fragment-based screening to identify starting points for drug discovery, and understanding and optimizing the pharmacological characteristics of GPCR-targeted drugs.

NMR support of fragment-based lead discovery.

Fragment-based screening (FBS) uses libraries of thousands of small molecular fragments to find starting points for developing novel drugs. This contrasts with high-throughput screening (HTS) of millions of compounds to find drug-sized starting compounds. Sampling of the chemical space tends to be more efficient with molecular fragments than with larger molecules, and as they form fewer interactions, small fragments bind to a wider range of sites on a greater number of proteins, leading to higher hit rates[188].

However, the binding affinities of small molecular fragments are likely to be lower than those for larger molecules, and therefore high assay sensitivity is needed in FBS. NMR spectroscopy was the first method used successfully to screen fragments[189], and it is still a commonly used method[17]. FBS has been applied to GPCRs with thermostabilization[190], and NMR has been utilized for FBS targeting β_1AR[191] and $A_{2A}AR$[192,193]. Ligand-observed NMR methods, such as target immobilized NMR screening (TINS) and saturation transfer difference spectroscopy (STD) (Fig. 8, a and b), have been utilized for FBS with β_1AR[191] and $A_{2A}AR$[192,193]; fragments have been identified that inhibited binding of tritium-labeled ligands with IC_{50} values ranging from 5 μM to 5 mM. Special advantages of these methods include that they can detect weak binders, require less protein than protein-observed NMR experiments, do not require isotope labels, and have no upper size limit for the protein[188,194]. The main challenge in FBS is in combining fragments to molecules for lead optimization, where structural information is required to decide on where to grow, merge or link a given fragment[195]. NMR methods can provide such information. Using forbidden coherence transfer (FCT) measurements[196], which is sensitive to the degree of surface complementarity, the substitution position of the ligands to grow can be identified. Transferred NOE spectroscopy[132,197,198] (Fig. 9c) and interligand NOEs for pharmacophore

mapping (INPHARMA)[135,199] (Fig. 9d) provide information about how to merge or link fragments in lead optimization processes. STD NMR[200–202] has also been applied for epitope mapping and determination of the bound conformations of GPCR ligands[203–206]. The bound conformations of ligands for kappa opioid receptor, pituitary adenylate cyclase activating polypeptide receptor, and leukotriene receptor BLT2 have been determined by transferred NOE spectroscopy[132,198,206], and INPHARMA has been applied for the generation of docking models of A_{2A}AR and GPR40[135,199].

NMR for optimization of drug pharmacological characteristics.

An attractive goal for structure-based drug design is to improve specificity of receptor–ligand interactions while increasing ligand affinities, efficacies and desired biased signaling. It has been proposed that structures of mutant GPCRs with increased thermostability in the agonist-bound state can be utilized for the development of agonists[4], and biased ligands of opioid receptors were identified by a structure-based approach[57,207], using inactive crystal structures in the antagonist-bound state. In this respect, NMR can provide structural information about conformational equilibria that are related to both the ligand efficacies and biased signaling in GPCRs. In addition, NMR studies revealed relationships between the chemical structures of GPCR ligands and their biased signaling, indicating that NMR studies would be helpful for the design of biased ligands.

For example, conformational changes of TMIII and TMVII in β_2AR that are not paralleled by those of TMV and TMVI in complexes with β-arrestin-biased ligands are in agreement with the following structure–activity relationships of β_2AR ligands (Fig. 9a and b). Modifications of the ethanolamine tail moieties, which are bound to TMIII and TMVII in the crystal structures[68,81,208], result in selective modulation of the efficacies for β-arrestin signaling, whereas modifications of the aromatic head groups, which bind to TMV and TMVI in the crystal structures[81,85,208], affect the efficacies of both G protein-mediated signaling and β-arrestin-mediated signaling[112]. Results from crystallography of the serotonin 5-HT_{1B} and 5-HT_{2B} receptors bound to ergotamine[209], and from fluorescence studies of the ghrelin receptor GHS-R1a[210] and the arginine vasopressin type 2 receptor[211] are also in agreement with selective activation of G protein- and β-arrestin-mediated signaling by localized conformational changes of TMV and TMVI, and of TMIII and TMVII, respectively.

In MOR, a comparison of olceridine derivatives, composed of the 2-[6-oxaspiro[4.5]decan-9-yl]ethylamine scaffold and two aromatic groups attached to the oxaspiro[4,5]decan and ethanolamine moieties (Fig. 9c), including compounds 6 to 11 and 13 to 19, revealed that the modification of either of the two aromatic rings results in selective modulation of β-arrestin signaling[164]. These structure–activity relationships of the olceridine derivatives are in agreement with a population shift of the conformational equilibria that accompanies the global conformational changes in TMIII, TMV, TMVI and TMVII upon the β-arrestin-biased N152A$^{3.35}$ mutation, as revealed by NMR (Fig. 9d)[129]. The coupled conformational changes of TMIII, TMV, TMVI and TMVII are also in agreement with the structure–activity relationships of the D_2 dopamine receptor: the modification of both the

head and tail groups of the ligands for D_2 dopamine receptor resulted in selective modulation of the β-arrestin signaling[212].

The mobility of the extracellular loops of GPCRs can affect the binding kinetics of ligands that attach to the binding pocket, and the binding kinetics correlates with the duration of drug action[78]. In molecular dynamics simulations of M2 and M3 muscarinic acetylcholine receptors bound to the ligand tiotropium, the ECL2 of the M3 receptor bound to tiotropium exhibited lower mobility than that of the M2 receptor[213]. The reduced mobility of the M3 receptor appears to parallel the slow association and dissociation of the ligand, and slow dissociation from the M3 receptor is responsible for the clinically preferable long-acting profile of tiotropium. In addition, ligands may adopt multiple different binding modes to their target molecules[214], and heterobivalent or non-bivalent ligands that are able to bind in two different orientations to the GPCRs have been identified for MOR, muscarinic M2 receptor, histamine H_1 receptor, and dopamine D3 receptor[215,216]. In the case of the bipharmacophoric ligands of muscarinic M2 receptor[216], consisting of an active moiety and an inactive moiety, the ligand binding modes dynamically switch between an active signaling-compotent pose and an inactive binding pose. The population of the active pose is related to the efficacies and is affected by the affinity ratio between the active and inactive moieties[216]. We conclude that dynamic ligand binding in multiple binding modes is a novel promising feature to be considered for the rational design of agonists with predictable efficacies. Finally, NMR has been utilized for investigations of the conformational equilibria in the ligand-binding sites of GPCRs[132], which are important for structure-guided drug design[217]. In the NMR study of kappa opioid receptor and its peptide ligand, motion on the sub-nanosecond timescale was observed for the N terminal region of the ligand, which is known to be crucial for activation[132]. Sub-nanosecond timescale motion in the ligand-binding site is correlated to the surface complementarity[196,218]; observation and optimization of ligand mobility thus promises to provide important input for the design of ligands with improved affinities.

Outlook

Since 2007, X-ray crystallography has set high standards for structure determination of human GPCR complexes with a wide range of drug molecules and other ligands, and the potential of cryo-EM to provide structure determinations of higher-order complexes of GPCRs, with ligands, modulators and partner proteins is now rapidly developing. While this review primarily discusses integrative use of X-ray crystal structures and NMR spectroscopy in solution, the inclusion of cryo-EM results is an exciting prospect, which may dominate the field in the future. Compared to X-ray crystallography, cryo-EM has greatly increased potential to provide structures of multiple simultaneously populated conformations in a given sample preparation[219]. It is exciting to look forward to combining this information on static arrays of different structures with the potential of solution NMR to characterize local and global three-dimensional structural polymorphisms in GPCRs, and to provide information on the relative populations of the different macromolecular species and the exchange kinetics among them.

In this review, we have emphasized the ability of NMR to study wild type or near-wild type GPCRs in aqueous media at physiological temperatures. For the future it will be important to further enable studies of GPCRs in sample preparations that also represent close mimics of other aspects of the physiological environment. In this context, the development of specialized, sophisticated GPCR biochemistry is called for. This may include the formation of lipid bilayer discs directly from cell membranes[220] or the preparation of size-controlled liposomes using a DNA nanotemplate[221], enabling NMR spectroscopy with GPCRs reconstituted in lipid mixtures that closely mimic those found in living cells. Combined with these improvements of GPCR reconstitution (Box 2), refined stable-isotope labeling (Box 1) will be needed, such as the use of non-native amino acids to introduce NMR probes at discrete locations in GPCRs expressed in mammalian or insect cells, and the use of segmental labeling for NMR studies of selected polypeptide segments in intact GPCRs[124]. However, refined GPCR biochemistry for NMR may come at the cost of lower expression and purification yields, and so the success of new approaches will also require advances in NMR technologies. Dynamic nuclear polarization (DNP) NMR, which can provide an orders-of-magnitude increase in experimental sensitivity for studies of challenging systems, appears particularly promising[222,223], and which has also been extensively used in solid state NMR[136,224–227].

Overall, there is the promise that NMR studies in solution environments that are ever closer to the physiological milieu will be used to investigate the structural basis of impacts by cellular traits on GPCR function[12]. Specifically, this will address phenomena such as GPCR oligomerization[228,229], posttranslational modifications[230], and complex formation with other partners such as receptor–activity modifying proteins (RAMP)[231]. Awaiting these technical advances and an abundance of new data from cryo-EM, we look forward to exciting times for the use of solution NMR in integrative GPCR structural biology projects. Each step forward in structural biology will support discovery of new drugs as well as improvement of existing drugs and their application.

Acknowledgements

This work is supported by The Ministry of Education, Culture, Sports, Science and Technology (MEXT)/Japan Society for the Promotion of Science (JSPS) KAKENHI Grant Numbers JP17H06097 (I.S.), JP18H04540 (T.U.), JP17H04999 (Y.K.); the development of core technologies for innovative drug development based upon IT and the development of innovative drug discovery technologies for middle-sized molecules, from the Japan Agency for Medical Research and Development, AMED (I.S.); an American Cancer Society Postdoctoral Fellowship (M.T.E); NIH/NIGMS R01GM115825 (K.W.); K.W. is the Cecil H. and Ida M. Green Professor of Structural Biology at The Scripps Research Institute

Glossary

Allosteric modulators

Molecules that bind to sites on GPCRs that are spatially distinct from the orthosteric binding pocket and modulate the affinity and/or efficacy of drugs bound to the orthosteric site. Allosteric modulators can be synthetic or endogenous compounds or metal ions in the cellular environment

Biased ligand

GPCR agonists can activate both G protein and β-arrestin signaling pathways (see Figure 1). Agonists that activate predominantly one of intracellular pathways are referred to as “biased ligands”. Drugs functioning as agonists may produce unwanted side effects mediated through the activation of multiple signaling pathways. Such side effects can be minimized by designing biased ligands that selectively activate only the signaling pathway required to produce the desired therapeutic response.

Conformational equilibria

Solution NMR studies established that GPCRs in near physiological environments exist in multiple, locally different conformers that are simultaneously populated in function-related equilibria. It has been shown that the relative populations of these conformers are related to the efficacies and the bias of bound drugs

GPCR Classes

GPCRs have been grouped into six different classes, labeled A through F, based on sequence homologies and physiological functions

Efficacy

Efficacy refers to the extent to which a GPCR ligand changes the receptor signaling intensity relative to its basal level. The efficacy is a key determinant of the therapeutic properties of a GPCR-targeting drug

Sequence motif

Polypeptide segments of 2 or several amino acids which are highly conserved among GPCRs of a given class and have been identified as key components of activation centers

Activation center

Clusters of closely spaced amino acids in the three-dimensional structure. Sequence motifs are often part of activation centers

Stable-isotope labeling

NMR spectroscopy with complex biomacromolecular systems is routinely based on labeling of proteins or other components with stable NMR-observable isotopes. Widely used stable isotopes in GPCR research are ^{2}H, ^{13}C, ^{15}N and ^{19}F

TROSY (transverse relaxation-optimized spectroscopy)

An experiment that enables solution NMR studies of large macromolecules or supramolecular structures, in particular of membrane proteins reconstituted into micelles, bicelles or nanodiscs

References

1. Rask-Andersen M, Almén MS & Schiöth HB Trends in the exploitation of novel drug targets. Nat. Rev. Drug Discov. 10, 579–590, doi:10.1038/nrd3478 (2011). [PubMed: 21804595]
2. Hauser AS, Attwood MM, Rask-Andersen M, Schiöth HB & Gloriam DE Trends in GPCR drug discovery: new agents, targets and indications. Nat. Rev. Drug Discov. 16, 829–842, doi:10.1038/nrd.2017.178 (2017). [PubMed: 29075003]
3. Santos R et al. A comprehensive map of molecular drug targets. Nat. Rev. Drug Discov. 16, 19–34, doi:10.1038/nrd.2016.230 (2017). [PubMed: 27910877]

4. Jazayeri A, Andrews SP & Marshall FH Structurally enabled discovery of adenosine A_{2A} receptor antagonists. Chem. Rev. 117, 21–37, doi:10.1021/acs.chemrev.6b00119 (2017). [PubMed: 27333206]
5. Hutchings CJ, Koglin M, Olson WC & Marshall FH Opportunities for therapeutic antibodies directed at G-protein-coupled receptors. Nat. Rev. Drug Discov. 16, 787–810, doi:10.1038/nrd.2017.91 (2017). [PubMed: 28706220]
6. Steyaert J & Kobilka BK Nanobody stabilization of G protein-coupled receptor conformational states. Curr. Opin. Struct. Biol. 21, 567–572, doi:10.1016/j.sbi.2011.06.011 (2011). [PubMed: 21782416]
7. Congreve M, Oswald C & Marshall FH Applying structure-based drug design approaches to allosteric modulators of GPCRs. Trends Pharmacol. Sci. 38, 837–847, doi:10.1016/j.tips.2017.05.010 (2017). [PubMed: 28648526]
8. Conn PJ, Lindsley CW, Meiler J & Niswender CM Opportunities and challenges in the discovery of allosteric modulators of GPCRs for treating CNS disorders. Nat. Rev. Drug Discov. 13, 692–708, doi:10.1038/nrd4308 (2014). [PubMed: 25176435]
9. Changeux J-P & Christopoulos A Allosteric Modulation as a Unifying Mechanism for Receptor Function and Regulation. Cell 166, 1084–1102, doi:10.1016/j.cell.2016.08.015 (2016). [PubMed: 27565340]
10. Changeux J-P 50 years of allosteric interactions: the twists and turns of the models. Nature reviews Molecular cell biology 14, 819 (2013). [PubMed: 24150612]
11. Violin JD, Crombie AL, Soergel DG & Lark MW Biased ligands at G-protein-coupled receptors: promise and progress. Trends Pharmacol. Sci. 35, 308–316 (2014). [PubMed: 24878326]
12. Smith JS, Lefkowitz RJ & Rajagopal S Biased signalling: from simple switches to allosteric microprocessors. Nat. Rev. Drug Discov, doi:10.1038/nrd.2017.229 (2018).
13. Lane JR, May LT, Parton RG, Sexton PM & Christopoulos A A kinetic view of GPCR allostery and biased agonism. Nat. Chem. Biol. 13, 929–937, doi:10.1038/nchembio.2431 (2017). [PubMed: 28820879]
14. Rankovic Z, Brust TF & Bohn LM Biased agonism: An emerging paradigm in GPCR drug discovery. Bioorg. Med. Chem. Lett. 26, 241–250, doi:10.1016/j.bmcl.2015.12.024 (2016). [PubMed: 26707396]
15. Reiter E, Ahn S, Shukla AK & Lefkowitz RJ Molecular mechanism of β-arrestin-biased agonism at seven-transmembrane receptors. Annu. Rev. Pharmacol. Toxicol. 52, 179–197 (2012). [PubMed: 21942629]
16. Ghosh E, Kumari P, Jaiman D & Shukla AK Methodological advances: the unsung heroes of the GPCR structural revolution. Nat. Rev. Mol. Cell Biol. 16, 69–81, doi:10.1038/nrm3933 (2015). [PubMed: 25589408]
17. Renaud JP et al. Biophysics in drug discovery: impact, challenges and opportunities. Nat. Rev. Drug Discov. 15, 679–698, doi:10.1038/nrd.2016.123 (2016). [PubMed: 27516170]
18. Didenko T, Liu JJ, Horst R, Stevens RC & Wüthrich K Fluorine-19 NMR of integral membrane proteins illustrated with studies of GPCRs. Curr. Opin. Struct. Biol. 23, 740–747, doi:10.1016/j.sbi.2013.07.011 (2013). [PubMed: 23932201]
19. Prosser RS & Kim TH Nuts and bolts of CF_3 and CH_3 NMR toward the understanding of conformational exchange of GPCRs. Methods Mol. Biol. 1335, 39–51, doi:10.1007/978-1-4939-2914-6_4 (2015). [PubMed: 26260593]
20. Ranjan R, Dwivedi H, Baidya M, Kumar M & Shukla AK Novel structural insights into GPCR-β-arrestin interaction and signaling. Trends Cell Biol. 27, 851–862, doi:10.1016/j.tcb.2017.05.008 (2017). [PubMed: 28651823]
21. Audet M & Bouvier M Restructuring G-protein- coupled receptor activation. Cell 151, 14–23, doi:10.1016/j.cell.2012.09.003 (2012). [PubMed: 23021212]
22. Wacker D, Stevens RC & Roth BL How ligands illuminate GPCR molecular pharmacology. Cell 170, 414–427, doi:10.1016/j.cell.2017.07.009 (2017). [PubMed: 28753422]
23. Wu F, Song G, de Graaf C & Stevens RC Structure and function of peptide-binding G protein-coupled receptors. J. Mol. Biol. 429, 2726–2745, doi:10.1016/j.jmb.2017.06.022 (2017). [PubMed: 28705763]

24. Hilger D, Masureel M & Kobilka BK Structure and dynamics of GPCR signaling complexes. Nat. Struct. Mol. Biol. 25, 4–12, doi:10.1038/s41594-017-0011-7 (2018). [PubMed: 29323277]
25. Carpenter B & Tate CG Active state structures of G protein-coupled receptors highlight the similarities and differences in the G protein and arrestin coupling interfaces. Curr. Opin. Struct. Biol. 45, 124–132, doi:10.1016/j.sbi.2017.04.010 (2017). [PubMed: 28482214]
26. Zhou XE, Melcher K & Xu HE Understanding the GPCR biased signaling through G protein and arrestin complex structures. Curr. Opin. Struct. Biol. 45, 150–159, doi:10.1016/j.sbi.2017.05.004 (2017). [PubMed: 28558341]
27. Scheerer P & Sommer ME Structural mechanism of arrestin activation. Curr. Opin. Struct. Biol. 45, 160–169, doi:10.1016/j.sbi.2017.05.001 (2017). [PubMed: 28600951]
28. Jazayeri A, Dias JM & Marshall FH From G Protein-coupled receptor structure resolution to rational drug design. J. Biol. Chem. 290, 19489–19495, doi:10.1074/jbc.R115.668251 (2015). [PubMed: 26100628]
29. Hauser AS et al. Pharmacogenomics of GPCR drug targets. Cell 172, 41–54.e19, doi:10.1016/j.cell.2017.11.033 (2018). [PubMed: 29249361]
30. Wootten D, Miller LJ, Koole C, Christopoulos A & Sexton PM Allostery and biased agonism at class B G protein-coupled receptors. Chem. Rev. 117, 111–138, doi:10.1021/acs.chemrev.6b00049 (2017). [PubMed: 27040440]
31. de Graaf C et al. Extending the structural view of class B GPCRs. Trends Biochem. Sci. 42, 946–960, doi:10.1016/j.tibs.2017.10.003 (2017). [PubMed: 29132948]
32. Renaud J-P et al. Cryo-EM in drug discovery: achievements, limitations and prospects. Nat. Rev. Drug Discov. (2018).
33. García-Nafría J, Nehmé R, Edwards PC & Tate CG Cryo-EM structure of the serotonin 5-HT1B receptor coupled to heterotrimeric Go. Nature 558, 620–623, doi:10.1038/s41586-018-0241-9 (2018). [PubMed: 29925951]
34. Kang Y et al. Cryo-EM structure of human rhodopsin bound to an inhibitory G protein. Nature 558, 553–558, doi:10.1038/s41586-018-0215-y (2018). [PubMed: 29899450]
35. Zhang Y et al. Cryo-EM structure of the activated GLP-1 receptor in complex with a G protein. Nature 546, 248–253, doi:10.1038/nature22394 (2017). [PubMed: 28538729]
36. Liang YL et al. Phase-plate cryo-EM structure of a class B GPCR-G-protein complex. Nature 546, 118–123, doi:10.1038/nature22327 (2017). [PubMed: 28437792]
37. Eddy MT & Yu T-Y Membranes, peptides, and disease: unraveling the mechanisms of viral proteins with solid state nuclear magnetic resonance spectroscopy. Solid state NMR 61–62, 1–7, doi:10.1016/j.ssnmr.2014.04.002 (2014).
38. Brown LS & Ladizhansky V Membrane proteins in their native habitat as seen by solid-state NMR spectroscopy. Protein Sci. 24, 1333–1346, doi:10.1002/pro.2700 (2015). [PubMed: 25973959]
39. Opella SJ & Marassi FM Applications of NMR to membrane proteins. Arch. Biochem. Biophys. 628, 92–101, doi:10.1016/j.abb.2017.05.011 (2017). [PubMed: 28529197]
40. Kaplan M, Pinto C, Houben K & Baldus M Nuclear magnetic resonance (NMR) applied to membrane–protein complexes. Q. Rev. Biophys. 49, 1010, doi:10.1017/S003358351600010X (2016).
41. Mandala VS, Williams JK & Hong M Structure and Dynamics of Membrane Proteins from Solid-State NMR. Annu. Rev. Biophys. 47, 201–222, doi:10.1146/annurev-biophys-070816-033712 (2018). [PubMed: 29498890]
42. Wylie BJ, Do HQ, Borcik CG & Hardy EP Advances in solid-state NMR of membrane proteins. Mol. Phys. 114, 3598–3609, doi:10.1080/00268976.2016.1252470 (2016).
43. Judge PJ & Watts A Recent contributions from solid-state NMR to the understanding of membrane protein structure and function. Curr. Opin. Chem. Biol. 15, 690–695, doi:10.1016/j.cbpa.2011.07.021 (2011). [PubMed: 21862384]
44. Alexander SP et al. THE CONCISE GUIDE TO PHARMACOLOGY 2017/18: G protein-coupled receptors. Br. J. Pharmacol. 174 Suppl 1, S17–S129, doi:10.1111/bph.13878 (2017). [PubMed: 29055040]

45. Bologna Z, Teoh JP, Bayoumi AS, Tang Y & Kim IM Biased G Protein-coupled receptor signaling: new player in modulating physiology and pathology. Biomol. Ther. (Seoul) 25, 12–25, doi: 10.4062/biomolther.2016.165 (2017). [PubMed: 28035079]
46. Benredjem B, Dallaire P & Pineyro G Analyzing biased responses of GPCR ligands. Curr. Opin. Pharmacol. 32, 71–76, doi:10.1016/j.coph.2016.11.008 (2017). [PubMed: 27930943]
47. Urban JD et al. Functional selectivity and classical concepts of quantitative pharmacology. J. Pharmacol. Exp. Ther. 320, 1–13 (2007). [PubMed: 16803859]
48. Pupo AS et al. Recent updates on GPCR biased agonism. Pharmacol. Res. 112, 49–57, doi: 10.1016/j.phrs.2016.01.031 (2016). [PubMed: 26836887]
49. Reiter E et al. β-arrestin signalling and bias in hormone-responsive GPCRs. Mol. Cell. Endocrinol. 449, 28–41, doi:10.1016/j.mce.2017.01.052 (2017). [PubMed: 28174117]
50. Thompson GL et al. Systematic analysis of factors influencing observations of biased agonism at the mu-opioid receptor. Biochem. Pharmacol. 113, 70–87, doi:10.1016/j.bcp.2016.05.014 (2016). [PubMed: 27286929]
51. Kenakin T Functional selectivity and biased receptor signaling. J. Pharmacol. Exp. Ther. 336, 296–302, doi:10.1124/jpet.110.173948 (2011). [PubMed: 21030484]
52. Soergel DG et al. First clinical experience with TRV130: pharmacokinetics and pharmacodynamics in healthy volunteers. J. Clin. Pharmacol. 54, 351–357 (2014). [PubMed: 24122908]
53. Soergel DG et al. Biased agonism of the μ-opioid receptor by TRV130 increases analgesia and reduces on-target adverse effects versus morphine: A randomized, double-blind, placebo-controlled, crossover study in healthy volunteers. Pain 155, 1829–1835 (2014). [PubMed: 24954166]
54. DeWire SM et al. A G protein-biased ligand at the μ-opioid receptor is potently analgesic with reduced gastrointestinal and respiratory dysfunction compared with morphine. J. Pharmacol. Exp. Ther. 344, 708–717 (2013). [PubMed: 23300227]
55. Schmid CL et al. Bias factor and therapeutic window correlate to predict safer opioid analgesics. Cell 171, 1165–1175.e1113, doi:10.1016/j.cell.2017.10.035 (2017). [PubMed: 29149605]
56. Majumdar S & Devi LA Strategy for making safer opioids bolstered. Nature 553, 286–288, doi: 10.1038/d41586-018-00045-1 (2018). [PubMed: 29345640]
57. Manglik A et al. Structure-based discovery of opioid analgesics with reduced side effects. Nature 537, 185–190, doi:10.1038/nature19112 (2016). [PubMed: 27533032]
58. Volkow ND & Collins FS The role of science in addressing the opioid crisis. N. Engl. J. Med. 377, 391–394, doi:10.1056/NEJMsr1706626 (2017). [PubMed: 28564549]
59. Sivertsen B, Holliday N, Madsen AN & Holst B Functionally biased signalling properties of 7TM receptors - opportunities for drug development for the ghrelin receptor. Br. J. Pharmacol. 170, 1349–1362, doi:10.1111/bph.12361 (2013). [PubMed: 24032557]
60. Rosenbaum DM, Rasmussen SG & Kobilka BK The structure and function of G-protein-coupled receptors. Nature 459, 356–363 (2009). [PubMed: 19458711]
61. Hanania NA, Dickey BF & Bond RA Clinical implications of the intrinsic efficacy of β-adrenoceptor drugs in asthma: full, partial and inverse agonism. Curr. Opin. Pulm. Med. 16, 1–5 (2010). [PubMed: 19887938]
62. Stotts AL, Dodrill CL & Kosten TR Opioid dependence treatment: options in pharmacotherapy. Expert Opin. Pharmacother. 10, 1727–1740, doi:10.1517/14656560903037168 (2009). [PubMed: 19538000]
63. Pich EM & Collo G Pharmacological targeting of dopamine D_3 receptors: Possible clinical applications of selective drugs. Eur. Neuropsychopharmacol. 25, 1437–1447, doi:10.1016/j.euroneuro.2015.07.012 (2015). [PubMed: 26298833]
64. Greene SJ et al. Partial adenosine A1 receptor agonism: a potential new therapeutic strategy for heart failure. Heart Fail Rev. 21, 95–102, doi:10.1007/s10741-015-9522-7 (2016). [PubMed: 26701329]
65. da Silva Junior ED et al. Factors influencing biased agonism in recombinant cells expressing the human α1A -adrenoceptor. Br. J. Pharmacol. 174, 2318–2333, doi:10.1111/bph.13837 (2017). [PubMed: 28444738]

66. Palczewski K et al. Crystal structure of rhodopsin: A G protein-coupled receptor. Science 289, 739–745 (2000). [PubMed: 10926528]
67. Rosenbaum DM et al. GPCR engineering yields high-resolution structural insights into β_2-adrenergic receptor function. Science 318, 1266–1273 (2007). [PubMed: 17962519]
68. Cherezov V et al. High-resolution crystal structure of an engineered human β_2-adrenergic G protein-coupled receptor. Science 318, 1258–1265 (2007). [PubMed: 17962520]
69. Pándy-Szekeres G et al. GPCRdb in 2018: adding GPCR structure models and ligands. Nucleic Acids Res. 46, D440–D446, doi:10.1093/nar/gkx1109 (2018). [PubMed: 29155946]
70. Draper-Joyce CJ et al. Structure of the adenosine-bound human adenosine A1 receptor–Gi complex. Nature 558, 559–563, doi:10.1038/s41586-018-0236-6 (2018). [PubMed: 29925945]
71. Koehl A et al. Structure of the μ-opioid receptor–Gi protein complex. Nature 558, 547–552, doi: 10.1038/s41586-018-0219-7 (2018). [PubMed: 29899455]
72. Ghosh E, Nidhi K & Shukla AK SnapShot: GPCR-ligand interactions. Cell 159, 1712, 1712.e1711, doi:10.1016/j.cell.2014.12.008 (2014). [PubMed: 25525884]
73. Zhang D et al. Two disparate ligand-binding sites in the human P2Y1 receptor. Nature 520, 317–321, doi:10.1038/nature14287 (2015). [PubMed: 25822790]
74. Jazayeri A et al. Extra-helical binding site of a glucagon receptor antagonist. Nature 533, 274–277, doi:10.1038/nature17414 (2016). [PubMed: 27111510]
75. Liu W et al. Structural basis for allosteric regulation of GPCRs by sodium ions. Science 337, 232–236, doi:10.1126/science.1219218 (2012). [PubMed: 22798613]
76. Fenalti G et al. Molecular control of δ-opioid receptor signalling. Nature 506, 191–196, doi: 10.1038/nature12944 (2014). [PubMed: 24413399]
77. Hanson MA et al. A specific cholesterol binding site is established by the 2.8 A structure of the human β_2-adrenergic receptor. Structure 16, 897–905, doi:10.1016/j.str.2008.05.001 (2008). [PubMed: 18547522]
78. Latorraca NR, Venkatakrishnan AJ & Dror RO GPCR dynamics: structures in motion. Chem. Rev. 117, 139–155, doi:10.1021/acs.chemrev.6b00177 (2017). [PubMed: 27622975]
79. Cong X, Topin J & Golebiowski J Class A GPCRs: structure, function, modeling and structure-based ligand design. Curr. Pharm. Des. 23, 4390–4409, doi: 10.2174/1381612823666170710151255 (2017). [PubMed: 28699533]
80. Tautermann CS GPCR structures in drug design, emerging opportunities with new structures. Bioorg. Med. Chem. Lett. 24, 4073–4079, doi:10.1016/j.bmcl.2014.07.009 (2014). [PubMed: 25086683]
81. Rasmussen SG et al. Structure of a nanobody-stabilized active state of the β_2 adrenoceptor. Nature 469, 175–180, doi:10.1038/nature09648 (2011). [PubMed: 21228869]
82. Ballesteros JA & Weinstein H Integrated methods for the construction of three-dimensional models and computational probing of structure-function relations in G-protein coupled receptors. Methods Neurosci. 25, 366–428 (1995).
83. Tehan BG, Bortolato A, Blaney FE, Weir MP & Mason JS Unifying family A GPCR theories of activation. Pharmacol. Ther. 143, 51–60, doi:10.1016/j.pharmthera.2014.02.004 (2014). [PubMed: 24561131]
84. Park JH, Scheerer P, Hofmann KP, Choe HW & Ernst OP Crystal structure of the ligand-free G-protein-coupled receptor opsin. Nature 454, 183–187 (2008). [PubMed: 18563085]
85. Rasmussen SG et al. Crystal structure of the β_2 adrenergic receptor-Gs protein complex. Nature 477, 549–555, doi:10.1038/nature10361 (2011). [PubMed: 21772288]
86. Manglik A & Kruse AC Structural basis for G Protein-coupled receptor activation. Biochemistry 56, 5628–5634, doi:10.1021/acs.biochem.7b00747 (2017). [PubMed: 28967738]
87. Kumari P, Ghosh E & Shukla AK Emerging approaches to GPCR ligand screening for drug discovery. Trends Mol. Med. 21, 687–701, doi:10.1016/j.molmed.2015.09.002 (2015). [PubMed: 26481827]
88. Zou Y, Weis WI & Kobilka BK N-terminal T4 lysozyme fusion facilitates crystallization of a G protein coupled receptor. PLoS One 7, e46039, doi:10.1371/journal.pone.0046039 (2012). [PubMed: 23056231]

89. Thompson AA et al. Structure of the nociceptin/orphanin FQ receptor in complex with a peptide mimetic. Nature 485, 395 (2012). [PubMed: 22596163]
90. Doré AS et al. Structure of the adenosine A_{2A} receptor in complex with ZM241385 and the xanthines XAC and caffeine. Structure 19, 1283–1293, doi:10.1016/j.str.2011.06.014 (2011). [PubMed: 21885291]
91. Lebon G, Bennett K, Jazayeri A & Tate CG Thermostabilisation of an agonist-bound conformation of the human adenosine A_{2A} receptor. J. Mol. Biol. 409, 298–310, doi:10.1016/j.jmb.2011.03.075 (2011). [PubMed: 21501622]
92. Warne T et al. The structural basis for agonist and partial agonist action on a β_1-adrenergic receptor. Nature 469, 241–244, doi:10.1038/nature09746 (2011). [PubMed: 21228877]
93. Carpenter B, Nehmé R, Warne T, Leslie AGW & Tate CG Structure of the adenosine A_{2A} receptor bound to an engineered G protein. Nature 536, 104–107, doi:10.1038/nature18966 (2016). [PubMed: 27462812]
94. Hino T et al. G-protein-coupled receptor inactivation by an allosteric inverse-agonist antibody. Nature 482, 237–240, doi:10.1038/nature10750 (2012). [PubMed: 22286059]
95. Warne T, Edwards PC, Leslie AG & Tate CG Crystal structures of a stabilized β_1-adrenoceptor bound to the biased agonists bucindolol and carvedilol. Structure 20, 841–849, doi:10.1016/j.str.2012.03.014 (2012). [PubMed: 22579251]
96. Zhang X, Stevens RC & Xu F The importance of ligands for G protein-coupled receptor stability. Trends Biochem. Sci. 40, 79–87, doi:10.1016/j.tibs.2014.12.005 (2015). [PubMed: 25601764]
97. Shihoya W et al. Activation mechanism of endothelin ET. Nature 537, 363–368, doi:10.1038/nature19319 (2016). [PubMed: 27595334]
98. White JF et al. Structure of the agonist-bound neurotensin receptor. Nature 490, 508–513, doi:10.1038/nature11558 (2012). [PubMed: 23051748]
99. Yang Z et al. Structural basis of ligand binding modes at the neuropeptide Y Y1 receptor. Nature, 1–22, doi:10.1038/s41586-018-0046-x (2018).
100. Mittermaier A & Kay L Observing biological dynamics at atomic resolution using NMR. Trends Biochem. Sci. 34, 601–611, doi:10.1016/j.tibs.2009.07.004 (2009). [PubMed: 19846313]
101. Osawa M, Takeuchi K, Ueda T, Nishida N & Shimada I Functional dynamics of proteins revealed by solution NMR. Curr. Opin. Struct. Biol. 22, 660–669, doi:10.1016/j.sbi.2012.08.007 (2012). [PubMed: 23000032]
102. Ikeya T et al. Solution NMR views of dynamical ordering of biomacromolecules. Biochim. Biophys. Acta 1862, 287–306, doi:10.1016/j.bbagen.2017.08.020 (2018).
103. Bhabha G et al. A dynamic knockout reveals that conformational fuctuations influence the chemical step of enzyme catalysis. Science 332, 234–238 (2011). [PubMed: 21474759]
104. Kerns SJ et al. The energy landscape of adenylate kinase during catalysis. Nat. Struct. Mol. Biol. 22, 124–131, doi:10.1038/nsmb.2941 (2015). [PubMed: 25580578]
105. Lange OF et al. Recognition dynamics up to microseconds revealed from an RDC-derived ubiquitin ensemble in solution. Science 320, 1471–1475, doi:10.1126/science.1157092 (2008). [PubMed: 18556554]
106. Morrison EA et al. Antiparallel EmrE exports drugs by exchanging between asymmetric structures. Nature 481, 45–50, doi:10.1038/nature10703 (2011). [PubMed: 22178925]
107. Brüschweiler S, Yang Q, Run C & Chou JJ Substrate-modulated ADP/ATP-transporter dynamics revealed by NMR relaxation dispersion. Nat. Struct. Mol. Biol. 22, 636–641, doi:10.1038/nsmb.3059 (2015). [PubMed: 26167881]
108. Minato Y et al. Conductance of $P2X_4$ purinergic receptor is determined by conformational equilibrium in the transmembrane region. Proc. Natl. Acad. Sci. U. S. A. 113, 4741–4746, doi:10.1073/pnas.1600519113 (2016). [PubMed: 27071117]
109. Nishida N et al. Functional dynamics of cell surface membrane proteins. J. Magn. Reson. 241, 86–96, doi:10.1016/j.jmr.2013.11.007 (2014). [PubMed: 24331735]
110. Pervushin K, Riek R, Wider G & Wüthrich K Attenuated T2 relaxation by mutual cancellation of dipole-dipole coupling and chemical shift anisotropy indicates an avenue to NMR structures of very large biological macromolecules in solution. Proc. Natl. Acad. Sci. U. S. A. 94, 12366–12371 (1997). [PubMed: 9356455]

111. Tugarinov V, Hwang PM, Ollerenshaw JE & Kay LE Cross-correlated relaxation enhanced ^{1}H-^{13}C NMR spectroscopy of methyl groups in very high molecular weight proteins and protein complexes. J. Am. Chem. Soc. 125, 10420–10428 (2003). [PubMed: 12926967]

112. Liu JJ, Horst R, Katritch V, Stevens RC & Wüthrich K Biased signaling pathways in β_2-adrenergic receptor characterized by ^{19}F-NMR. Science 335, 1106–1110, doi:10.1126/science.1215802 (2012). [PubMed: 22267580]

113. Kofuku Y et al. Efficacy of the β_2-adrenergic receptor is determined by conformational equilibrium in the transmembrane region. Nat. Commun. 3, 1045, doi:10.1038/ncomms2046 (2012). [PubMed: 22948827]

114. Isogai S et al. Backbone NMR reveals allosteric signal transduction networks in the β1-adrenergic receptor. Nature 530, 237–241, doi:10.1038/nature16577 (2016). [PubMed: 26840483]

115. Solt AS et al. Insight into partial agonism by observing multiple equilibria for ligand-bound and Gs-mimetic nanobody-bound β1-adrenergic receptor. Nat. Commun. 8, 1795, doi:10.1038/s41467-017-02008-y (2017). [PubMed: 29176642]

116. Bokoch MP et al. Ligand-specific regulation of the extracellular surface of a G-protein-coupled receptor. Nature 463, 108–112 (2010). [PubMed: 20054398]

117. Chung KY et al. Role of detergents in conformational exchange of a G protein-coupled receptor. J. Biol. Chem. 287, 36305–36311, doi:10.1074/jbc.M112.406371 (2012). [PubMed: 22893704]

118. Nygaard R et al. The dynamic process of β_2-adrenergic receptor activation. Cell 152, 532–542, doi:10.1016/j.cell.2013.01.008 (2013). [PubMed: 23374348]

119. Kim TH et al. The role of ligands on the equilibria between functional states of a G protein-coupled receptor. J. Am. Chem. Soc. 135, 9465–9474, doi:10.1021/ja404305k (2013). [PubMed: 23721409]

120. Horst R, Liu JJ, Stevens RC & Wüthrich K β_2-adrenergic receptor activation by agonists studied with ^{19}F NMR spectroscopy. Angew. Chem. Int. Ed. Engl. 52, 10762–10765, doi:10.1002/anie.201305286 (2013). [PubMed: 23956158]

121. Kofuku Y et al. Functional dynamics of deuterated β_2-adrenergic receptor in lipid bilayers revealed by NMR spectroscopy. Angew. Chem. Int. Ed. 53, 13376–13379, doi:10.1002/anie.201406603 (2014).

122. Manglik A et al. Structural insights into the dynamic process of β_2-adrenergic receptor signaling. Cell 161, 1101–1111, doi:10.1016/j.cell.2015.04.043 (2015). [PubMed: 25981665]

123. Eddy MT, Didenko T, Stevens RC & Wüthrich K β_2-adrenergic receptor conformational response to fusion protein in the third intracellular loop. Structure 24, 2190–2197, doi:10.1016/j.str.2016.09.015 (2016). [PubMed: 27839952]

124. Shiraishi Y et al. Phosphorylation-induced conformation of β_2-adrenoceptor related to arrestin recruitment revealed by NMR. Nat. Commun. 9, 194, doi:10.1038/s41467-017-02632-8 (2018). [PubMed: 29335412]

125. Ye L, Van Eps N, Zimmer M, Ernst OP & Prosser RS Activation of the A_{2A} adenosine G-protein-coupled receptor by conformational selection. Nature 533, 265–268, doi:10.1038/nature17668 (2016). [PubMed: 27144352]

126. Clark LD et al. Ligand modulation of sidechain dynamics in a wild-type human GPCR. Elife 6, doi:10.7554/eLife.28505 (2017).

127. Eddy MT et al. Allosteric coupling of drug binding and intracellulars signaling in the A_{2A} adenosine receptor. Cell 172, 68–80.e12, doi:10.1016/j.cell.2017.12.004 (2018). [PubMed: 29290469]

128. Sounier R et al. Propagation of conformational changes during μ-opioid receptor activation. Nature 524, 375–378, doi:10.1038/nature14680 (2015). [PubMed: 26245377]

129. Okude J et al. Identification of a conformational equilibrium that determines the efficacy and functional selectivity of the μ-opioid receptor. Angew. Chem. Int. Ed. Engl. 54, 15771–15776, doi:10.1002/anie.201508794 (2015). [PubMed: 26568421]

130. Casiraghi M et al. Functional modulation of a G protein-coupled receptor conformational landscape in a lipid bilayer. J. Am. Chem. Soc. 138, 11170–11175, doi:10.1021/jacs.6b04432 (2016). [PubMed: 27489943]

131. Ye L et al. Mechanistic insights into allosteric regulation of the A_{2A} adenosine G protein-coupled receptor by physiological cations. Nat. Commun. 9, 1372, doi:10.1038/s41467-018-03314-9 (2018). [PubMed: 29636462]
132. O'Connor C et al. NMR structure and dynamics of the agonist dynorphin peptide bound to the human kappa opioid receptor. Proc. Natl. Acad. Sci. U. S. A. 112, 11852–11857, doi:10.1073/pnas.1510117112 (2015). [PubMed: 26372966]
133. Park SH, Berkamp S, Radoicic J, De Angelis AA & Opella SJ Interaction of monomeric interleukin-8 with CXCR1 mapped by proton-detected fast MAS solid-state NMR. Biophys. J. 113, 2695–2705, doi:10.1016/j.bpj.2017.09.041 (2017). [PubMed: 29262362]
134. Berkamp S, Park SH, De Angelis AA, Marassi FM & Opella SJ Structure of monomeric Interleukin-8 and its interactions with the N-terminal Binding Site-I of CXCR1 by solution NMR spectroscopy. J. Biomol. NMR 69, 111–121, doi:10.1007/s10858-017-0128-3 (2017). [PubMed: 29143165]
135. Bartoschek S et al. Drug design for G-protein-coupled receptors by a ligand-based NMR method. Angew. Chem. 49, 1426–1429, doi:10.1002/anie.200905102 (2010). [PubMed: 20084646]
136. Joedicke L et al. The molecular basis of subtype selectivity of human kinin G-protein-coupled receptors. Nat. Chem. Biol. 14, 284–290, doi:10.1038/nchembio.2551 (2018). [PubMed: 29334381]
137. Goricanec D et al. Conformational dynamics of a G-protein α subunit is tightly regulated by nucleotide binding. Proc. Natl. Acad. Sci. U. S. A. 113, E3629–3638, doi:10.1073/pnas.1604125113 (2016). [PubMed: 27298341]
138. Toyama Y et al. Dynamic regulation of GDP binding to G proteins revealed by magnetic field-dependent NMR relaxation analyses. Nat. Commun. 8, 14523, doi:10.1038/ncomms14523 (2017). [PubMed: 28223697]
139. Zhuang T et al. Involvement of distinct arrestin-1 elements in binding to different functional forms of rhodopsin. Proc. Natl. Acad. Sci. U. S. A. 110, 942–947, doi:10.1073/pnas.1215176110 (2013). [PubMed: 23277586]
140. London RE, Wingad BD & Mueller GA Dependence of amino acid side chain ^{13}C shifts on dihedral angle: application to conformational analysis. J. Am. Chem. Soc. 130, 11097–11105 (2008). [PubMed: 18652454]
141. Butterfoss GL et al. Conformational dependence of ^{13}C shielding and coupling constants for methionine methyl groups. J. Biomol. NMR 48, 31–47 (2010). [PubMed: 20734113]
142. Perkins SJ & Wüthrich K Ring current effects in the conformation dependent NMR chemical shifts of aliphatic protons in the basic pancreatic trypsin inhibitor. Biochim. Biophys. Acta 576, 409–423 (1979). [PubMed: 427198]
143. Liu D & Wüthrich K Ring current shifts in ^{19}F-NMR of membrane proteins. J. Biomol. NMR 65, 1–5, doi:10.1007/s10858-016-0022-4 (2016). [PubMed: 27240587]
144. Pintacuda G & Otting G Identification of protein surfaces by NMR measurements with a pramagnetic Gd(III) chelate. J. Am. Chem. Soc. 124, 372–373 (2002). [PubMed: 11792196]
145. Bloembergen N, Purcell EM & Pound RV Relaxation effects in nuclear magnetic resonance absorption. Phys. Rev. 73, 679–712, doi:10.1103/PhysRev.73.679 (1948).
146. Staus DP et al. Allosteric nanobodies reveal the dynamic range and diverse mechanisms of G-protein-coupled receptor activation. Nature 535, 448–452, doi:10.1038/nature18636 (2016). [PubMed: 27409812]
147. Gether U et al. Agonists induce conformational changes in transmembrane domains III and VI of the β_2 adrenoceptor. EMBO J. 16, 6737–6747 (1997). [PubMed: 9362488]
148. Ghanouni P, Steenhuis JJ, Farrens DL & Kobilka BK Agonist-induced conformational changes in the G-protein-coupling domain of the β_2 adrenergic receptor. Proc. Natl. Acad. Sci. U. S. A. 98, 5997–6002, doi:10.1073/pnas.101126198 (2001). [PubMed: 11353823]
149. Yao X et al. Coupling ligand structure to specific conformational switches in the β_2-adrenoceptor. Nat. Chem. Biol. 2, 417–422 (2006). [PubMed: 16799554]
150. Yao XJ et al. The effect of ligand efficacy on the formation and stability of a GPCR-G protein complex. Proc. Natl. Acad. Sci. U. S. A. 106, 9501–9506 (2009). [PubMed: 19470481]

151. Gregorio GG et al. Single-molecule analysis of ligand efficacy in β_2AR-G-protein activation. Nature 547, 68–73, doi:10.1038/nature22354 (2017). [PubMed: 28607487]
152. Lamichhane R et al. Single-molecule view of basal activity and activation mechanisms of the G protein-coupled receptor β_2AR. Proc. Natl. Acad. Sci. U. S. A. 112, 14254–14259, doi:10.1073/pnas.1519626112 (2015). [PubMed: 26578769]
153. Stumpf AD & Hoffmann C Optical probes based on G protein-coupled receptors - added work or added value? Br. J. Pharmacol. 173, 255–266, doi:10.1111/bph.13382 (2016). [PubMed: 26562218]
154. Rahmeh R et al. Structural insights into biased G protein-coupled receptor signaling revealed by fluorescence spectroscopy. Proc. Natl. Acad. Sci. U. S. A. 109, 6733–6738 (2012). [PubMed: 22493271]
155. Kahsai AW et al. Multiple ligand-specific conformations of the β_2-adrenergic receptor. Nat. Chem. Biol. 7, 692–700 (2011). [PubMed: 21857662]
156. Xiao K, Chung J & Wall A The power of mass spectrometry in structural characterization of GPCR signaling. J. Recept. Signal Transduct. Res. 35, 213–219, doi:10.3109/10799893.2015.1072979 (2015). [PubMed: 26459735]
157. West GM et al. Ligand-dependent perturbation of the conformational ensemble for the GPCR β_2 adrenergic receptor revealed by HDX. Structure 19, 1424–1432 (2011). [PubMed: 21889352]
158. Wisler JW et al. A unique mechanism of beta-blocker action: carvedilol stimulates beta-arrestin signaling. Proc. Natl. Acad. Sci. U. S. A. 104, 16657–16662, doi:10.1073/pnas.0707936104 (2007). [PubMed: 17925438]
159. Drake MT et al. β-arrestin-biased agonism at the β_2-adrenergic receptor. J. Biol. Chem. 283, 5669–5676, doi:10.1074/jbc.M708118200 (2008). [PubMed: 18086673]
160. Carr R et al. β-arrestin-biased signaling through the β_2-adrenergic receptor promotes cardiomyocyte contraction. Proc. Natl. Acad. Sci. U. S. A. 113, E4107–4116, doi:10.1073/pnas.1606267113 (2016). [PubMed: 27354517]
161. Imai S et al. Functional equilibrium of the KcsA structure revealed by NMR. J. Biol. Chem. 287, 39634–39641, doi:10.1074/jbc.M112.401265 (2012). [PubMed: 23024361]
162. Boom M et al. Non-analgesic effects of opioids: opioid-induced respiratory depression. Curr. Pharm. Des. 18, 5994–6004 (2012). [PubMed: 22747535]
163. Dahan A et al. Anesthetic potency and influence of morphine and sevoflurane on respiration in μ-opioid receptor knockout mice. Anesthesiology 94, 824–832 (2001). [PubMed: 11388534]
164. Chen XT et al. Structure-activity relationships and discovery of a G protein biased μ opioid receptor ligand, [(3-methoxythiophen-2-yl)methyl]({2-[(9R)-9-(pyridin-2-yl)-6-oxaspiro-[4.5]decan- 9-yl]ethyl})amine (TRV130), for the treatment of acute severe pain. J. Med. Chem. 56, 8019–8031 (2013). [PubMed: 24063433]
165. Huang W et al. Structural insights into μ-opioid receptor activation. Nature 524, 315–321, doi:10.1038/nature14886 (2015). [PubMed: 26245379]
166. Manglik A et al. Crystal structure of the μ-opioid receptor bound to a morphinan antagonist. Nature 485, 321–326 (2012). [PubMed: 22437502]
167. Ferré S et al. Adenosine A_{2A} receptors in ventral striatum, hypothalamus and nociceptive circuitry implications for drug addiction, sleep and pain. Prog. Neurobiol. 83, 332–347, doi:10.1016/j.pneurobio.2007.04.002 (2007). [PubMed: 17532111]
168. Schiffmann SN, Fisone G, Moresco R, Cunha RA & Ferré S Adenosine A_{2A} receptors and basal ganglia physiology. Prog. Neurobiol. 83, 277–292, doi:10.1016/j.pneurobio.2007.05.001 (2007). [PubMed: 17646043]
169. Young A et al. Co-inhibition of CD73 and A2AR adenosine signaling improves anti-tumor immune responses. Cancer Cell 30, 391–403, doi:10.1016/j.ccell.2016.06.025 (2016). [PubMed: 27622332]
170. Hatfield SM & Sitkovsky M A2A adenosine receptor antagonists to weaken the hypoxia-HIF-1α driven immunosuppression and improve immunotherapies of cancer. Curr. Opin. Pharmacol. 29, 90–96, doi:10.1016/j.coph.2016.06.009 (2016). [PubMed: 27429212]

171. Leone RD, Lo YC & Powell JD A2aR antagonists: Next generation checkpoint blockade for cancer immunotherapy. Comput. Struct. Biotechnol. J. 13, 265–272, doi:10.1016/j.csbj.2015.03.008 (2015). [PubMed: 25941561]

172. Mediavilla-Varela M et al. Antagonism of adenosine A2A receptor expressed by lung adenocarcinoma tumor cells and cancer associated fibroblasts inhibits their growth. Cancer Biol. Ther. 14, 860–868, doi:10.4161/cbt.25643 (2013). [PubMed: 23917542]

173. Mittal D et al. Antimetastatic effects of blocking PD-1 and the adenosine A2A receptor. Cancer Res. 74, 3652–3658, doi:10.1158/0008-5472.CAN-14-0957 (2014). [PubMed: 24986517]

174. Jaakola VP et al. The 2.6 angstrom crystal structure of a human A_{2A} adenosine receptor bound to an antagonist. Science 322, 1211–1217 (2008). [PubMed: 18832607]

175. Xu F et al. Structure of an agonist-bound human A_{2A} adenosine receptor. Science 332, 322–327 (2011). [PubMed: 21393508]

176. Lebon G et al. Agonist-bound adenosine A_{2A} receptor structures reveal common features of GPCR activation. Nature 474, 521–525 (2011). [PubMed: 21593763]

177. Carpenter B, Nehmé R, Warne T, Leslie AG & Tate CG Structure of the adenosine A_{2A} receptor bound to an engineered G protein. Nature 536, 104–107, doi:10.1038/nature18966 (2016). [PubMed: 27462812]

178. Sušac L, O'Connor C, Stevens RC & Wüthrich K In-Membrane Chemical Modification (IMCM) for site-specific chromophore labeling of GPCRs. Angew. Chem. Int. Ed. Engl. 54, 15246–15249, doi:10.1002/anie.201508506 (2015). [PubMed: 26545333]

179. Susac L NMR studies of GPCR structure and function Ph. D. thesis, The Scripps Research Institute, (2015).

180. Piirainen H et al. Human adenosine A_{2A} receptor binds calmodulin with high affinity in a calcium-dependent manner. Biophys. J. 108, 903–917, doi:10.1016/j.bpj.2014.12.036 (2015). [PubMed: 25692595]

181. Tossavainen H, Hellman M, Piirainen H, Jaakola V & Permi P H-N, N, C-a, C-β and C' assignments of the intrinsically disordered C-terminus of human adenosine A_{2A} receptor. Biomol. NMR Assign. 9, 403–406, doi:10.1007/s12104-015-9618-y (2015). [PubMed: 25952762]

182. Venkatakrishnan AJ et al. Structured and disordered facets of the GPCR fold. Curr. Opin. Struct. Biol. 27, 129–137, doi:10.1016/j.sbi.2014.08.002 (2014). [PubMed: 25198166]

183. Berlow RB, Dyson HJ & Wright PE Expanding the paradigm: intrinsically disordered proteins and allosteric regulation. J. Mol. Biol, doi:10.1016/j.jmb.2018.04.003 (2018).

184. Wright PE & Dyson HJ Intrinsically disordered proteins in cellular signalling and regulation. Nature 16, 18–29, doi:10.1038/nrm3920 (2015).

185. Oh DY & Olefsky JM G protein-coupled receptors as targets for anti-diabetic therapeutics. Nat. Rev. Drug Discov. 15, 161–172, doi:10.1038/nrd.2015.4 (2016). [PubMed: 26822831]

186. Prasad-Reddy L & Isaacs D A clinical review of GLP-1 receptor agonists: efficacy and safety in diabetes and beyond. Drugs Context 4, 212283, doi:10.7573/dic.212283 (2015). [PubMed: 26213556]

187. Hou Y et al. Solvent-accessibility of discrete residue positions in the polypeptide hormone glucagon by ^{19}F-NMR observation of 4-fluorophenylalanine. J. Biomol. NMR 68, 1–6, doi:10.1007/s10858-017-0107-8 (2017). [PubMed: 28508109]

188. Erlanson DA, Fesik SW, Hubbard RE, Jahnke W & Jhoti H Twenty years on: the impact of fragments on drug discovery. Nature Rev. Drug Discov. 15, 605–619, doi:10.1038/nrd.2016.109 (2016). [PubMed: 27417849]

189. Shuker SB, Hajduk PJ, Meadows RP & Fesik SW Discovering high-affinity ligands for proteins: SAR by NMR. Science 274, 1531–1534 (1996). [PubMed: 8929414]

190. Andrews SP, Brown GA & Christopher JA Structure-Based and Fragment-Based GPCR Drug Discovery. ChemMedChem 9, 256–275, doi:10.1002/cmdc.201300382 (2013). [PubMed: 24353016]

191. Congreve M et al. Fragment screening of stabilized G-protein-coupled receptors using biophysical methods. Methods Enzymol. 493, 115–136, doi:10.1016/B978-0-12-381274-2.00005-4 (2011). [PubMed: 21371589]

192. Chen D et al. Fragment screening of GPCRs using biophysical methods: identification of ligands of the adenosine A_{2A} receptor with novel biological activity. ACS Chem. Biol. 7, 2064–2073, doi:10.1021/cb300436c (2012). [PubMed: 23013674]

193. Igonet S et al. Enabling STD-NMR fragment screening using stabilized native GPCR: A case study of adenosine receptor. Sci. Rep. 8, 8142, doi:10.1038/s41598-018-26113-0 (2018). [PubMed: 29802269]

194. Pellecchia M, Sem DS & Wüthrich K NMR in drug discovery. Nat. Rev. Drug Discov. 1, 211–219, doi:10.1038/nrd748 (2002). [PubMed: 12120505]

195. Hajduk PJ & Greer J A decade of fragment-based drug design: strategic advances and lessons learned. Nat. Rev. Drug Discov. 6, 211–219, doi:10.1038/nrd2220 (2007). [PubMed: 17290284]

196. Mizukoshi Y et al. Improvement of ligand affinity and thermodynamic properties by NMR-based evaluation of local dynamics and surface complementarity in the receptor-bound state. Angew. Chem. 55, 14606–14609 (2016). [PubMed: 27762089]

197. Brancaccio D et al. Ligand-Based NMR Study of C-X-C Chemokine Receptor Type 4 (CXCR4)–Ligand Interactions on Living Cancer Cells. J. Med. Chem. 61, 2910–2923, doi:10.1021/acs.jmedchem.7b01830 (2018). [PubMed: 29522685]

198. Inooka H et al. Conformation of a peptide ligand bound to its G-protein coupled receptor. Nat. Struct. Biol. 8, 161–165, doi:10.1038/84159 (2001). [PubMed: 11175907]

199. Fredriksson K et al. Nanodiscs for INPHARMA NMR characterization of GPCRs: ligand binding to the Human A_{2A} adenosine receptor. Angew. Chem. Int. Ed. Engl. 56, 5750–5754, doi:10.1002/anie.201612547 (2017). [PubMed: 28429411]

200. Cox BD et al. Structural analysis of CXCR4 - Antagonist interactions using saturation-transfer double-difference NMR. Biochem. Biophys. Res. Commun. 466, 28–32, doi:10.1016/j.bbrc.2015.08.084 (2015). [PubMed: 26301631]

201. Yong KJ et al. Determinants of ligand subtype-selectivity at α_{1A}-adrenoceptor revealed using saturation transfer difference (STD) NMR. ACS Chem. Biol. 13, 1090–1102, doi:10.1021/acschembio.8b00191 (2018). [PubMed: 29537256]

202. Assadi-Porter FM et al. Direct NMR detection of the binding of functional ligands to the human sweet receptor, a heterodimeric family 3 GPCR. J. Am. Chem. Soc. 130, 7212–7213, doi:10.1021/ja8016939 (2008). [PubMed: 18481853]

203. Kofuku Y et al. Structural Basis of the Interaction between Chemokine Stromal Cell-derived Factor-1/CXCL12 and Its G-protein-coupled Receptor CXCR4. J. Biol. Chem. 284, 35240–35250, doi:10.1074/jbc.M109.024851 (2009). [PubMed: 19837984]

204. Yoshiura C et al. Elucidation of the CCR1- and CCR5-binding modes of MIP-1α by application of an NMR spectra reconstruction method to the transferred cross-saturation experiments. J. Biomol. NMR 63, 333–340, doi:10.1007/s10858-015-9992-x (2015). [PubMed: 26472202]

205. Yoshiura C et al. NMR analyses of the interaction between CCR5 and its ligand using functional reconstitution of CCR5 in lipid bailayers. J. Am. Chem. Soc. 132, 6768–6777, doi:10.1021/ja100830f (2010). [PubMed: 20423099]

206. Catoire LJ et al. Structure of a GPCR ligand in its receptor-bound state: leukotriene B4 adopts a highly constrained conformation when associated to human BLT2. J. Am. Chem. Soc. 132, 9049–9057, doi:10.1021/ja101868c (2010). [PubMed: 20552979]

207. Zheng Z et al. Structure-based discovery of new antagonist and biased agonist chemotypes for the kappa opioid receptor. J. Med. Chem. 60, 3070–3081, doi:10.1021/acs.jmedchem.7b00109 (2017). [PubMed: 28339199]

208. Ring AM et al. Adrenaline-activated structure of β_2-adrenoceptor stabilized by an engineered nanobody. Nature 502, 575–579, doi:10.1038/nature12572 (2013). [PubMed: 24056936]

209. Wacker D et al. Structural features for functional selectivity at serotonin receptors. Science 340, 615–619 (2013). [PubMed: 23519215]

210. Mary S et al. Ligands and signaling proteins govern the conformational landscape explored by a G protein-coupled receptor. Proc. Natl. Acad. Sci. U S A 109, 8304–8309 (2012). [PubMed: 22573814]

211. Rahmeh R et al. Structural insights into biased G protein-coupled receptor signaling revealed by fluorescence spectroscopy. Proc. Natl. Acad. Sci. U S A 109, 6733–6738 (2012). [PubMed: 22493271]
212. Shonberg J et al. A structure-activity analysis of biased agonism at the dopamine D_2 receptor. J. Med. Chem. 56, 9199–9221, doi:10.1021/jm401318w (2013). [PubMed: 24138311]
213. Kruse AC et al. Structure and dynamics of the M3 muscarinic acetylcholine receptor. Nature 482, 552–556, doi:10.1038/nature10867 (2012). [PubMed: 22358844]
214. Lewi PJ et al. On the detection of multiple-binding modes of ligands to proteins, from biological, structural, and modeling data. J. Comput. Aided Mol. Des. 17, 129–134 (2003). [PubMed: 13677481]
215. Wittmann HJ & Strasser A Competitive association binding kinetic assays: a new tool to detect two different binding orientations of a ligand to its target protein under distinct conditions? Naunyn Schmiedebergs Arch. Pharmacol. 390, 595–612, doi:10.1007/s00210-017-1362-7 (2017). [PubMed: 28220211]
216. Bock A et al. Dynamic ligand binding dictates partial agonism at a G protein-coupled receptor. Nat. Chem. Biol. 10, 18–20, doi:10.1038/nchembio.1384 (2014). [PubMed: 24212135]
217. Bruchas MR & Roth BL New technologies for elucidating opioid receptor function. Trends Pharmacol. Sci. 37, 279–289, doi:10.1016/j.tips.2016.01.001 (2016). [PubMed: 26833118]
218. Sharp KA, O'Brien E, Kasinath V & Wand AJ On the relationship between NMR-derived amide order parameters and protein backbone entropy changes. Proteins: Struct., Funct., Bioinf. 83, 922–930 (2015).
219. Renaud J-P et al. Cryo-EM in drug discovery: achievements, limitations and prospects. Nat. Rev. Drug Discov. 17, 471–492, doi:10.1038/nrd.2018.77 (2018). [PubMed: 29880918]
220. Yasuhara K et al. Spontaneous lipid nanodisc fomation by amphiphilic polymethacrylate copolymers. J. Am. Chem. Soc. 139, 18657–18663, doi:10.1021/jacs.7b10591 (2017). [PubMed: 29171274]
221. Yang Y et al. Self-assembly of size-controlled liposomes on DNA nanotemplates. Nat. Chem. 8, 476–483, doi:10.1038/nchem.2472 (2016). [PubMed: 27102682]
222. Zhang G & Hilty C Applications of dissolution dynamic nuclear polarization in chemistry and biochemistry. Mag. Res. Chem. 56, 566–582, doi:10.1002/mrc.4735 (2018).
223. Ragavan M, Chen H-Y, Sekar G & Hilty C Solution NMR of Polypeptides Hyperpolarized by Dynamic Nuclear Polarization. Analyt. Chem. 83, 6054–6059, doi:10.1021/ac201122k (2011). [PubMed: 21651293]
224. Bajaj VS, Mak-Jurkauskas ML, Belenky M, Herzfeld J & Griffin RG Functional and shunt states of bacteriorhodopsin resolved by 250 GHz dynamic nuclear polarization-enhanced solid-state NMR. Proc. Natl. Acad. Sci. U. S. A. 106, 9244–9249, doi:10.1073/pnas.0900908106 (2009). [PubMed: 19474298]
225. Mak-Jurkauskas ML et al. Energy transformations early in the bacteriorhodopsin photocycle revealed by DNP-enhanced solid-state NMR. Proc. Natl. Acad. Sci. U. S. A. 105, 883–888, doi: 10.1073/pnas.0706156105 (2008). [PubMed: 18195364]
226. Ni QZ et al. Primary Transfer Step in the Light-Driven Ion Pump Bacteriorhodopsin: An Irreversible U-Turn Revealed by Dynamic Nuclear Polarization-Enhanced Magic Angle Spinning NMR. J. Am. Chem. Soc. 140, 4085–4091, doi:10.1021/jacs.8b00022 (2018). [PubMed: 29489362]
227. Frederick KK et al. Sensitivity-Enhanced NMR Reveals Alterations in Protein Structure by Cellular Milieus. Cell 163, 620–628, doi:10.1016/j.cell.2015.09.024 (2015). [PubMed: 26456111]
228. George SR, O'Dowd BF & Lee SP G-Protein-coupled receptor oligomerization and its potential for drug discovery. Nat. Rev. Drug Discov. 1, 808–820, doi:10.1038/nrd913 (2002). [PubMed: 12360258]
229. Gurevich VV & Gurevich EV GPCRs and Signal Transducers: Interaction Stoichiometry. Trends Pharmacol. Sci. 39, 672–684, doi:10.1016/j.tips.2018.04.002 (2018). [PubMed: 29739625]

230. Nørskov-Lauritsen L & Bräuner-Osborne H Role of post-translational modifications on structure, function and pharmacology of class C G protein-coupled receptors. Eur. J. Pharmacol. 763, 233–240, doi:10.1016/j.ejphar.2015.05.015 (2015). [PubMed: 25981296]

231. Klein KR, Matson BC & Caron KM The expanding repertoire of receptor activity modifying protein (RAMP) function. Crit. Rev. Biochem. Mol. Biol. 51, 65–71, doi: 10.3109/10409238.2015.1128875 (2015).

232. Zhang H et al. Structure of the full-length glucagon class B G-protein-coupled receptor. Nature 546, 259–264, doi:10.1038/nature22363 (2017). [PubMed: 28514451]

233. Zhang X et al. Crystal structure of a multi-domain human smoothened receptor in complex with a super stabilizing ligand. Nat. Commun. 8, 15383, doi:10.1038/ncomms15383 (2017). [PubMed: 28513578]

234. Noguchi S & Satow Y Purification of human β_2-adrenergic receptor expressed in methylotrophic yeast *Pichia pastoris*. J. Biochem. 140, 799–804, doi:10.1093/jb/mvj211 (2006). [PubMed: 17050613]

235. Krettler C, Reinhart C & Bevans CG Expression of GPCRs in *Pichia pastoris* for structural studies. Methods Enzymol. 520, 1–29, doi:10.1016/B978-0-12-391861-1.00001-0 (2013). [PubMed: 23332693]

236. Yurugi-Kobayashi T et al. Comparison of functional non-glycosylated GPCRs expression in *Pichia pastoris*. Biochem. Biophys. Res. Commun. 380, 271–276, doi:10.1016/j.bbrc. 2009.01.053 (2009). [PubMed: 19167344]

237. Shimamura T et al. Structure of the human histamine H1 receptor complex with doxepin. Nature 475, 65–70, doi:10.1038/nature10236 (2011). [PubMed: 21697825]

238. Eddy MT et al. Extrinsic tryptophans as NMR probes of allosteric coupling in membrane proteins: application to the A2A adenosine receptor. J. Am. Chem. Soc. 140, 8228–8235, doi: 10.1021/jacs.8b03805 (2018). [PubMed: 29874058]

239. Klein-Seetharaman J, Getmanova EV, Loewen MC, Reeves PJ & Khorana HG NMR spectroscopy in studies of light-induced structural changes in mammalian rhodopsin: applicability of solution ^{19}F NMR. Proc. Natl. Acad. Sci. U. S. A. 96, 13744–13749 (1999). [PubMed: 10570143]

240. Otting G Protein NMR using paramagnetic ions. Annu. Rev. Biophys. 39, 387–405, doi:10.1146/ annurev.biophys.093008.131321 (2010). [PubMed: 20462377]

241. Clore GM & Iwahara J Theory, practice, and applications of paramagnetic relaxation enhancement for the characterization of transient low-population states of biological macromolecules and their complexes. Chem. Rev. 109, 4108–4139, doi:10.1021/cr900033p (2009). [PubMed: 19522502]

242. Iwahara J, Tang C & Clore G Practical aspects of ^{1}H transverse paramagnetic relaxation enhancement measurements on macromolecules. J. Mag. Reson. 184, 185–195, doi:10.1016/ j.jmr.2006.10.003 (2007).

243. Su X-C & Otting G Paramagnetic labelling of proteins and oligonucleotides for NMR. J. Biomol. NMR 46, 101–112, doi:10.1007/s10858-009-9331-1 (2009). [PubMed: 19529883]

244. Huang S et al. Utilization of paramagnetic relaxation enhancements for structural analysis of actin-binding proteins in complex with actin. Sci. Rep. 6, 33690, doi:10.1038/srep33690 (2016). [PubMed: 27654858]

245. Salzmann M, Wider G, Pervushin K, Senn H & Wüthrich K TROSY-type triple-resonance experiments for sequential NMR assignments of large proteins. J. Am. Chem. Soc. 121, 844–848, doi:10.1021/ja9834226 (1999).

246. Clark L et al. Methyl labeling and TROSY NMR spectroscopy of proteins expressed in the eukaryote *Pichia pastoris*. J. Biomol. NMR 62, 239–245, doi:10.1007/s10858-015-9939-2 (2015). [PubMed: 26025061]

247. Opitz C, Isogai S & Grzesiek S An economic approach to efficient isotope labeling in insect cells using homemade ^{15}N-, ^{13}C- and ^{2}H-labeled yeast extracts. J. Biomol. NMR 62, 373–385, doi: 10.1007/s10858-015-9954-3 (2015). [PubMed: 26070442]

248. Franke B et al. Production of isotope-labeled proteins in insect cells for NMR. J. Biomol. NMR 22, 1583–1512, doi:10.1007/s10858-018-0172-7 (2018).

249. Kofuku Y et al. Deuteration and selective labeling of alanine methyl groups of β_2-adrenergic receptor expressed in a baculovirus-insect cell expression system. J. Biomol. NMR, doi:10.1007/s10858-018-0174-5 (2018).
250. Huber T, Naganathan S, Tian H, Ye S & Sakmar TP Unnatural amino acid mutagenesis of GPCRs using amber codon suppression and bioorthogonal labeling. Methods Enzymol. 520, 281–305, doi:10.1016/B978-0-12-391861-1.00013-7 (2013). [PubMed: 23332705]
251. Grunbeck A, Huber T, Sachdev P & Sakmar TP Mapping the ligand-binding site on a G protein-coupled receptor (GPCR) using genetically encoded photocrosslinkers. Biochemistry 50, 3411–3413, doi:10.1021/bi200214r (2011). [PubMed: 21417335]
252. Daggett KA & Sakmar TP Site-specific *in vitro* and *in vivo* incorporation of molecular probes to study G-protein-coupled receptors. Curr. Opin. Chem. Biol. 15, 392–398, doi:10.1016/j.cbpa.2011.03.010 (2011). [PubMed: 21571577]
253. Ye S et al. Tracking G-protein-coupled receptor activation using genetically encoded infrared probes. Nature 464, 1386–1389, doi:10.1038/nature08948 (2010). [PubMed: 20383122]
254. Egloff P et al. Structure of signaling-competent neurotensin receptor 1 obtained by directed evolution in Escherichia coli. Proc. Natl. Acad. Sci. U. S. A. 111, E655–662, doi:10.1073/pnas.1317903111 (2014). [PubMed: 24453215]
255. Casiraghi M, Damian M, Lescop E, Banères J-L & Catoire LJ Illuminating the energy landscape of GPCRs: the key contribution of solution-state NMR associated with Escherichia coli as an expression host. Biochemistry 57, 2297–2307, doi:10.1021/acs.biochem.8b00035 (2018). [PubMed: 29607648]
256. Maly J & Crowhurst KA Expression, purification and preliminary NMR characterization of isotopically labeled wild-type human heterotrimeric G protein α_{i1}. Protein Expr. Purif. 84, 255–264, doi:10.1016/j.pep.2012.06.003 (2012). [PubMed: 22713620]
257. Sounier R, Yang Y, Hagelberger J, Granier S & Déméné H ^{1}H, ^{13}C, and ^{15}N backbone chemical shift assignments of camelid single-domain antibodies against active state μ -opioid receptor. Biomol. NMR Assign. 11, 117–121, doi:10.1007/s12104-017-9733-z (2017). [PubMed: 28239762]
258. Dawaliby R et al. Allosteric regulation of G protein-coupled receptor activity by phospholipids. Nat. Chem. Biol. 12, 35–39, doi:10.1038/nchembio.1960 (2016). [PubMed: 26571351]
259. Pei G, Tiberi M, Caron MG & Lefkowitz RJ An approach to the study of G-protein-coupled receptor kinases: an in vitro-purified membrane assay reveals differential receptor specificity and regulation by G beta gamma subunits. Proc. Natl. Acad. Sci. U. S. A. 91, 3633–3636 (1994). [PubMed: 8170959]
260. Bayburt TH, Grinkova YV & Sligar SG Self-assembly of discoidal phospholipid bilayer nanoparticles with membrane scaffold proteins. Nano Lett. 2, 853–856, doi:10.1021/nl025623k (2002).
261. Denisov IG & Sligar SG Nanodiscs in membrane biochemistry and biophysics. Chem. Rev. 117, 4669–4713, doi:10.1021/acs.chemrev.6b00690 (2017). [PubMed: 28177242]
262. Denisov IG, Grinkova YV, Lazarides AA & Sligar SG Directed self-assembly of monodisperse phospholipid bilayer Nanodiscs with controlled size. J. Am. Chem. Soc. 126, 3477–3487, doi:10.1021/ja0393574 (2004). [PubMed: 15025475]
263. Leitz AJ, Bayburt TH, Barnakov AN, Springer BA & Sligar SG Functional reconstitution of β_2-adrenergic receptors utilizing self-assembling Nanodisc technology. BioTechniques 40, 601–602, 604, 606, passim (2006). [PubMed: 16708760]
264. Bocquet N et al. Real-time monitoring of binding events on a thermostabilized human A_{2A} receptor embedded in a lipid bilayer by surface plasmon resonance. Biochim. Biophys. Acta 1848, 1224–1233, doi:10.1016/j.bbamem.2015.02.014 (2015). [PubMed: 25725488]
265. Van Eps N et al. Conformational equilibria of light-activated rhodopsin in nanodiscs. Proc. Natl. Acad. Sci. U. S. A. 114, E3268–E3275, doi:10.1073/pnas.1620405114 (2017). [PubMed: 28373559]
266. Dijkman PM & Watts A Lipid modulation of early G protein-coupled receptor signalling events. Biochim. Biophys. Acta 1848, 2889–2897, doi:10.1016/j.bbamem.2015.08.004 (2015). [PubMed: 26275588]

267. Bayburt TH et al. Monomeric rhodopsin is sufficient for normal rhodopsin kinase (GRK1) phosphorylation and arrestin-1 binding. J. Biol. Chem. 286, 1420–1428 (2011). [PubMed: 20966068]

268. Inagaki S et al. Modulation of the interaction between neurotensin receptor NTS1 and Gq protein by lipid. J. Mol. Biol. 417, 95–111, doi:10.1016/j.jmb.2012.01.023 (2012). [PubMed: 22306739]

269. Mitra N et al. Calcium-dependent ligand binding and G-protein signaling of family B GPCR parathyroid hormone 1 receptor purified in nanodiscs. ACS Chem. Biol. 8, 617–625, doi: 10.1021/cb300466n (2013). [PubMed: 23237450]

270. El Moustaine D et al. Distinct roles of metabotropic glutamate receptor dimerization in agonist activation and G-protein coupling. Proc. Natl. Acad. Sci. U. S. A. 109, 16342–16347, doi: 10.1073/pnas.1205838109 (2012). [PubMed: 22988116]

271. Schuler MA, Denisov IG & Sligar SG Nanodiscs as a new tool to examine lipid-protein interactions. Methods Mol. Biol. 974, 415–433, doi:10.1007/978-1-62703-275-9_18 (2013). [PubMed: 23404286]

272. Nasr ML et al. Covalently circularized nanodiscs for studying membrane proteins and viral entry. Nat. Methods 14, 49–52, doi:10.1038/nmeth.4079 (2017). [PubMed: 27869813]

273. Chien CH et al. An adaptable phospholipid membrane mimetic system for solution NMR studies of membrane proteins. J. Am. Chem. Soc. 139, 14829–14832, doi:10.1021/jacs.7b06730 (2017). [PubMed: 28990386]

274. Frauenfeld J et al. A saposin-lipoprotein nanoparticle system for membrane proteins. Nat. Methods 13, 345–351, doi:10.1038/nmeth.3801 (2016). [PubMed: 26950744]

275. Orwick MC et al. Detergent-free formation and physicochemical characterization of nanosized lipid-polymer complexes: Lipodisq. Angew. Chem. Int. Ed. Engl. 51, 4653–4657, doi:10.1002/anie.201201355 (2012). [PubMed: 22473824]

276. Shi L et al. β_2 adrenergic receptor activation. Modulation of the proline kink in transmembrane 6 by a rotamer toggle switch. J. Biol. Chem. 277, 40989–40996, doi:10.1074/jbc.M206801200 (2002). [PubMed: 12167654]

277. Schwartz TW, Frimurer TM, Holst B, Rosenkilde MM & Elling CE Molecular mechanism of 7TM receptor activation--a global toggle switch model. Annu. Rev. Pharmacol. Toxicol. 46, 481–519, doi:10.1146/annurev.pharmtox.46.120604.141218 (2006). [PubMed: 16402913]

Box 1 |

Preparation of native-like human GPCRs for solution NMR

Expression systems

Protein production for most published GPCR NMR studies has been carried out using insect cell-baculovirus expression systems (BVES), which are also routinely used for protein production in GPCR crystallography. More recently, mammalian cell cultures have been employed for expression of GPCRs with large extracellular domains, as typically found in Class B and Class F GPCRs[232,233], which also retain human-like glycosylation and other post-translational modifications. Several human GPCRs have also been recombinantly expressed in yeast, particularly in *Pichia pastoris*[234–236], including the histamine H1 receptor[237] and adenosine A_{2A} receptor (A_{2A}AR)[238]. A survey of expression systems used for the preparation of GPCR NMR samples is included in Table 1.

Labeling by post-translational chemical modification

Many GPCR NMR studies so far introduced NMR probes by chemical modification of amino acid side chains during or after protein production. This strategy benefits from the comparatively high expression yields for wild type-like GPCRs, since NMR probes are incorporated in a post-translational step during protein purification at specific locations in the receptor through chemical conjugation to reactive –SH or $–NH_3$ groups of amino acid side chains. Two common extrinsic GPCR NMR probes are ^{19}F-groups chemically conjugated with cysteines, and $^{13}CH_3$ groups introduced by reductive methylation of lysines. The use of trifluoromethyl probes in integral membrane proteins was pioneered by Khorana for NMR studies of bovine rhodopsin[239], and more recently applied to studies of β_2AR[112,117,119,120,122] and A_{2A}AR[125,131]. Methylated lysines have been used in NMR studies of β_2AR[116] and MOR[128].

Introduction of NMR probes by chemical modification has made use both of targeting suitably located endogenous cysteines or lysines and of amino acid replacement in judiciously selected sequence locations with non-endogenous cysteines[125,178]. Generally, post-translational chemical modification is limited to residues at the extracellular or intracellular surfaces; however, unintended labeling of non-surface residues can occur, creating unwanted background signals that interfere with the interpretation of NMR data from the surface-facing probes. For example, in A_{2A}AR the labeling of a cysteine engineered into the intracellular surface resulted in heterogeneous labeling of additional cysteines when the protein was solubilized in detergent micelles. To overcome this problem, the in-membrane chemical modification (IMCM) method was introduced, whereby ^{19}F NMR probes are chemically introduced into GPCRs embedded in membranes isolated from the expression host, i.e., before protein isolation and purfication[178]. Alternatively, ^{19}F-NMR background signals have been removed by replacement of all but the cysteine(s) of interest by other amino acids.

Post-translational chemical modification has also been used to introduce paramagnetic relaxation enhancement (PRE) agents, such as nitroxide spin labels, into discrete

sequence locations in proteins[240–242]. This approach has been widely used in NMR structure determination efforts and studies of intermolecular interactions of soluble and membrane proteins[240,243,244], using cysteine-modifying chemistry similar to the ^{19}F-NMR approach to introduce such spin labels at discrete locations in GPCRs.

Expression in stable-isotope labeled media

Stable isotopes can be used in the cell culture medium for GPCR production, either as stable-isotope-labeled amino acids, such as $^{13}CH_3$-methionine[113,115,118,121,129] and ^{15}N-valine[114], or stable-isotope-labeled nutrients, where ^{15}N, ^{13}C, and ^{2}H are then incorporated uniformly throughout the receptor[127].

Deuteration of GPCRs is necessary to obtain the full benefits of high resolution in [^{15}N, ^{1}H]-TROSY correlation NMR experiments[110,245]. Expression of deuterated GPCRs in eukaryotic organisms has historically been a challenge, as insect and mammalian cells do not tolerate D_2O, but deuteration of human GPCRs has been achieved by protein production with *Pichia pastoris* in D_2O media[126,127,246]. Higher levels of protein deuteration were achieved by adding deuterated carbon sources[126,246]. Illustrations for successful expression in *Pichia pastoris* include deuterated human A_{2A}AR, enabling of ^{13}C-methyl labeling of isoleucines[126,246], and studies of ^{1}H–^{15}N backbone and side chain signals[127]. A limitation of deuteration by expression of human GPCRs in *P. pastoris* grown in D_2O media is that back-protonation of amide groups can be incomplete, resulting in a smaller number of NMR signals than one would expect from the amino acid sequence. Deuteration in insect cells and mammalian cells has been achieved by introducing deuterated amino acids or deuterated digests from lower organisms to the cell culture media. Examples are the expression of deuterated GPCRs in BVES by introducing deuterated amino acids in H_2O-based insect cell media for β_2AR[121] and MOR[129], and the use of H_2O-based insect cell media containing deuterated yeast digests for expression of β_1AR[247] and the C-C chemokine receptor type 5 (CCR5)[248]. Using these approaches, the extent of deuteration may be lower than what is achieved with D_2O-based expression media for *P. pastoris*, but back-protonation is expected to be nearly complete[247]. Selective $^{13}CH_3$ labeling of alanine methyl groups on a deuterated background has been achieved for β_2AR expressed in BVES[249].

Introduction of non-proteinogenic amino acids through amber codon suppression technology has been used to introduce NMR probes into GPCRs for residue-specific biophysical characterization of dynamics and ligand binding events[250–253]. Using this approach, ^{19}F NMR probes such as fluorotyrosine can be introduced at specific interior locations in transmembrane helices that are inaccessible for post-translational chemical modification.

Expression of human GPCRs in *E. coli*, which is the standard expression system for stable-isotope labeled proteins for NMR studies, has so far found limited applications[130,254,255].

Labeling of GPCR ligands and partner proteins

Expression of the isotopically labeled Gα subunit of the trimeric G protein complex has been carried out in *E. coli*, permitting deuteration and uniform or amino acid-specific

labeling of G proteins[256]. Isotopically labeled G protein mimicking camelid single-chain antibodies, so-called “nanobodies,” for the μ-opioid receptor (MOR) have also been expressed and characterized by solution NMR[257].

Box 2 |

Reconstitution of human GPCRs for NMR studies in solution

Under physiological conditions, GPCRs are embedded in lipid bilayers, whereas for structural studies they have so far in most cases been solubilized by detergents. In detergent micelles, GPCRs do not necessarily retain their full activities[258], and a lipid bilayer environment is reportedly preferable for GPCR phosphorylation by GRKs[259]. Nanodiscs can accommodate membrane proteins within a 10-nm-diameter disc-shaped lipid bilayer, stabilized by α-helical amphipathic membrane scaffold proteins (MSPs)[260,261]. Nanodiscs thus promise to provide a lipid environment with more native-like properties in terms of the lateral pressure and curvature profiles, since detergent micelles have a strong curvature and different lateral pressure profiles from lipid membranes[262]. Membrane proteins embedded in nanodiscs are attractive for investigating interacting ligands on one side and signaling partner proteins on the other side. Nanodiscs are water soluble and monodisperse, which has already enabled their use in various GPCR studies[121,124,130,151,152,204,205,258,263–271].

Nasr et al. recently reported covalently circularized nanodiscs (cNDs) with enhanced stability and strictly defined diameter sizes, which are obtained by circularizing the MSP using sortase[272]. The NMR spectra of a β-barrel membrane protein, VDAC-1, embedded in cNDs exhibited enhanced signal intensities and spectral resolution due to reduced sample heterogeneity[272], suggesting that cNDs could facilitate future NMR analyses of GPCRs in lipid bilayers. Disc-shaped lipid bilayers have also been formed using the saposin-A scaffold protein (Salipro nanoparticles[273,274]) or synthetic polymers[220,275]. Saposin-A scaffold proteins are reportedly helpful for the formation of bilayer discs with different sizes, and the synthetic polymer discs have the advantage of being formed directly from lipid bilayers, without using detergents.

Under physiological conditions, GPCRs can be embedded in the lipid bilayers of tissues with various lipid compositions, and the signaling activities of GPCRs can be affected by the lipid composition of the bilayers. For example, experimental studies using β_2AR in nanodiscs indicated that phospholipids can act as allosteric modulators[258], and the NMR signals of leukotriene B4 receptor in nanodiscs were found to be affected by the addition of cholesteryl hemisuccinate[130]. Reconstitution of GPCRs into nanodisc lipid bilayers thus opens avenues to examine effects of various composition of lipid bilayers on the activities and conformational equilibria of GPCRs by solution NMR experiments at near-physiological temperatures.

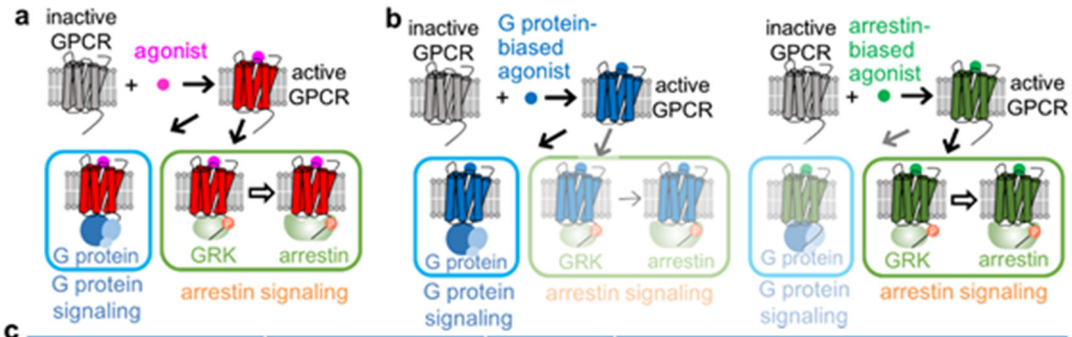

c

Biased ligands	Target	Bias	Therapeutics
TRV027, TRV120023	angiotensin II type-1 receptor	arrestin	antihypertensive effect with cardioprotection
oliceridine, TRV734	μ opioid receptor	G protein	analgesics with reduced tolerance
TRV250	δ opioid receptor	G protein	anti-migraine drug with reduced seizure

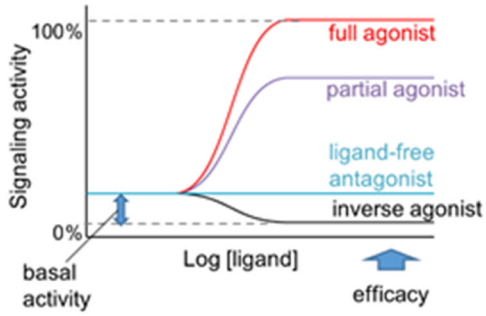

e

Partial agonists	Target	Therapeutic use	References
capadenoson	adenosine A_1 receptor	hemodynamically neutral heart failure	*Heart Fail Rev.* (2016) **21**, 95-102
aripiperazole	dopamine D_2 receptor	dopamine system stabilizer	*Eur. J. Pharmacol.* (2015) **752**, 112-115
tulobuterol, clenbuterol	β_2 adrenergic receptor	treatment of chronic asthma	*Curr. Opin. Pulm. Med.* (2010) **16**, 1-5
buprenorphine	μ opioid receptor	opioid dependence	*Exp. Opin. Pharmacol.* (2009) **10**, 1727-1740

Figure 1 |. Therapeutic use, efficacy, and biased signaling of GPCR ligands.

a | Schematic diagram of GPCR signaling. Activated GPCRs induce signal transduction through independent signaling pathways, either *via* G proteins or *via* G protein-coupled receptor kinases (GRKs) and arrestins. **b** | Schematic diagram of biased signaling. A G protein-biased ligand and an arrestin-biased ligand elicit signaling *via* the G protein pathway and the arrestin pathway, respectively. **c** | Examples of clinically effective biased ligands of GPCRs. **d** | Plots of signaling activity *versus* ligand concentration, representing different common GPCR efficacies. **e** | Examples of clinically effective partial agonists of GPCRs.

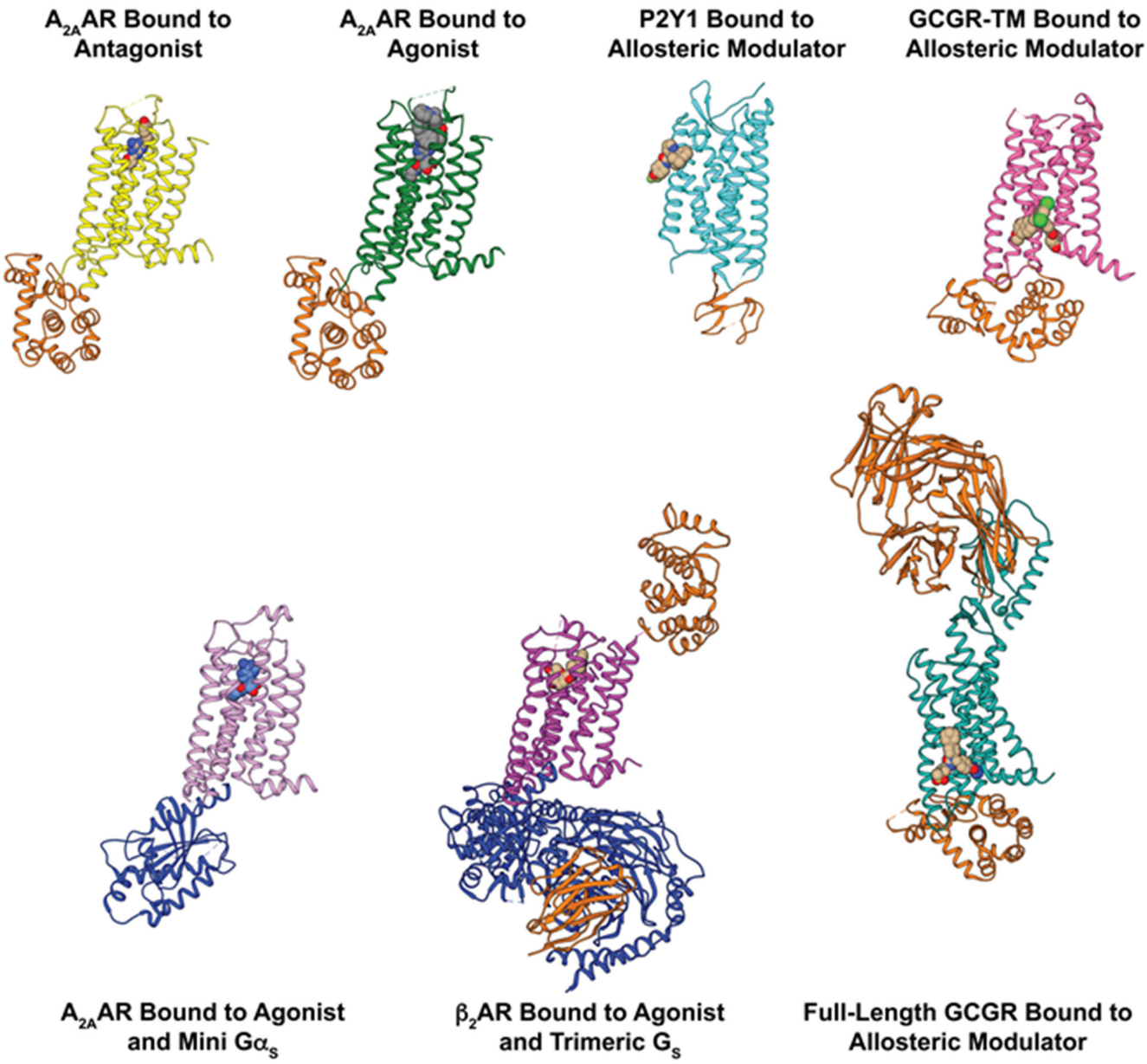

Figure 2 |. Selected crystallography data on GPCR structural architectures and intermolecular interactions.

Side views are shown of crystal structures of GPCRs in binary complexes with orthosteric ligands or allosteric modulators, and in tertiary complexes with intracellular partner proteins and orthosteric ligands or allosteric modulators. Fusion proteins, nanobodies, and antibodies used to facilitate crystallization of the GPCR complexes are shown in orange, and intracellular partner proteins are shown in blue. Different colors are used for different functional states of GPCRs: A_{2A}AR in complex with the antagonist ZM241385 (yellow; PDB 3EML) and the agonist UK432097 (green; PDB 3QAK), P2Y1 receptor bound to the allosteric modulator BPTU (cyan; PDB 4XNV), the transmembrane domain (TM) of GCGR in complex with the allosteric modulator MK-0893 (fuchsia; PDB 5EE7), A_{2A}AR in a

tertiary complex with the agonist NECA and a mini Gs protein (salmon; PDB 5G53), β_2AR in a tertiary complex with an agonist and a heterotrimeric G protein (purple; PDB 3SN6), and full-length GCGR in complex with the allosteric modulator NNC0640 (marine; PDB 5XEZ).

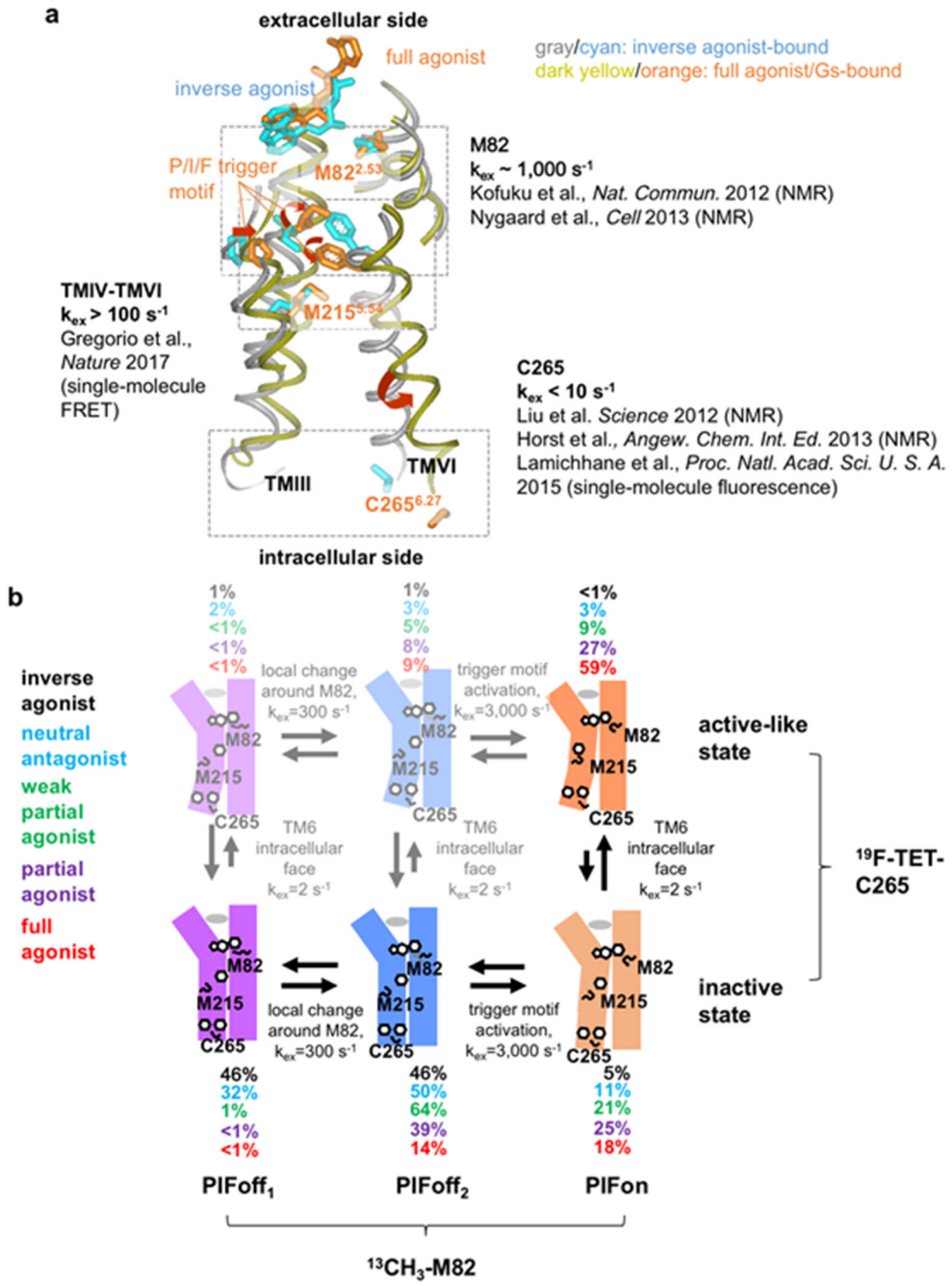

Figure 3 |. Conformational plasticity of β_2AR.

a | Exchange rates between simultaneously populated locally different conformations observed with NMR and fluorescence probes introduced in different locations of β_2AR. Shown are the crystal structures of β_2AR complexes with the inverse agonist carazolol (PDB: 2RH1), and with the full agonist BI-167107 and a G-protein (PDB: 3SN6), overlaid for best fit of TMII; the drawing represents a side view with the extracellular surface at the top. TMII, TMIII, TMV and TMVI are shown as grey or dark-yellow C^{α} traces, and the sidechains of M82$^{2.53}$, I121$^{3.40}$, P211$^{5.50}$, M215$^{5.54}$, C265$^{6.27}$ and F282$^{6.44}$, and the bound

ligands are depicted by cyan or orange sticks, as detailed in the figure. The antagonist and full agonist complexes differ by a rearrangement of the TM helices and the P/I/F activation motif of $P211^{5.50}$, $I121^{3.40}$ and $F282^{6.44}$. The rearrangement at the P/I/F motif induces conformational changes near the cytoplasmic region that is involved in G protein binding. The environments around $M82^{2.53}$, $M215^{5.54}$, and $C265^{6.27}$ have been shown to be sensitive to the above-described conformational changes upon activation. **b** | Schematic model of plasticity in β_2AR, which rationalizes the wide range of different exchange rates in (**a**). Vertical arrows indicate the equilibria between 'inactive' and 'active-like' conformations at the cytoplasmic surface, as observed with NMR probes at C265. Horizontal arrows correspond to equilibria in the local region around M82 ($PIFoff_1 \leftrightarrow PIFoff_2$) and in the P/I/F motif ($PIFoff_2 \leftrightarrow PIFon$), as observed with probes at M82 (the states $PIFoff_1$, $PIFoff_2$ and PIFon correspond to $M82^D$, $M82^U$ and $M82^A$ in a previous report[113]). Black, cyan, green, purple and red numbers are the populations of the different states, as observed experimentally for β_2AR bound to an inverse agonist, an antagonist, a weak partial agonist, a partial agonist, and a full agonist, respectively. The states with populations below 10% are listed in faint colors.

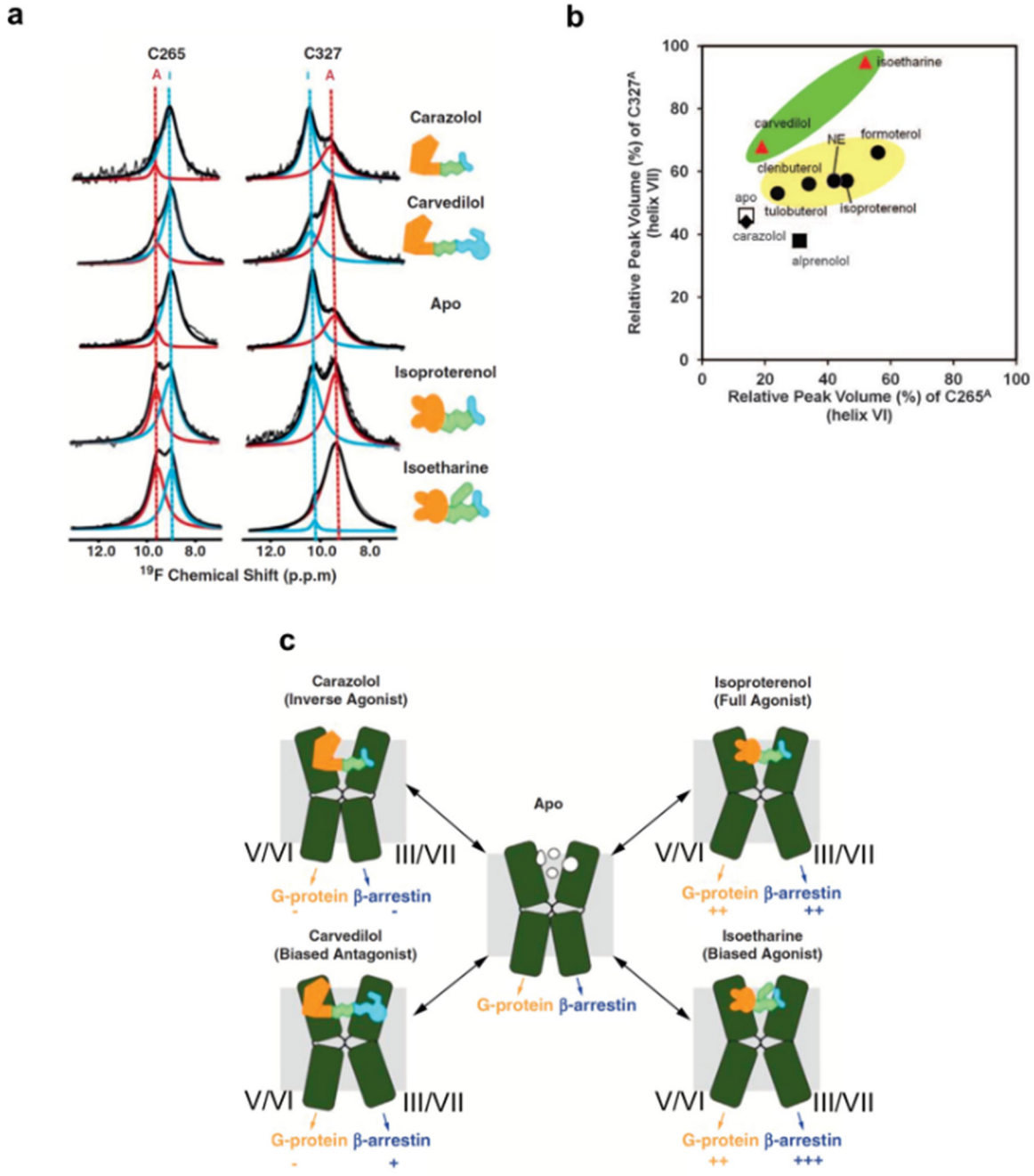

Figure 4 |. NMR-observable conformational equilibria related to biased signaling of β_2AR.

a | ^{19}F-NMR signals of CF_3 probes attached to C265 and C327 in the apo-form and in four drug complexes of β_2AR. The experimental spectra (thin black line showing noise) have been deconvoluted into signals of an active-like state (red, A) and an inactive state (blue, I) of β_2AR. The thick black line represents the sum of the signals I and A. **b** | Plot of the relative peak volumes for an active-like state of β_2AR observed at C265 ($C265^A$) versus the relative peak volumes for an active-like state at C327 ($C327^A$). The relative peak volumes are the ratios of the volume of peak A and the sum of the volumes of peaks A and I. The

data for the complexes with the agonists tulobuterol, clenbuterol, norepinephrine (NE), isoproterenol, and formoterol are shown as black circles highlighted by a yellow background. The data with the biased ligands carvedilol and isoetharine are shown as red triangles highlighted by a green background. The data with the neutral antagonist alprenolol, the inverse agonist carazolol, and the apo state are shown as a black square, a black diamond, and an open square, respectively. **c** | Signaling intensities through two β_2AR pathways suggested by the ^{19}F-NMR experiments. TMVI and TMVII of β_2AR are shown as green kinked cylinders. The structures of the four bound ligands are schematically drawn (yellow, green, and cyan) and their functionalities are indicated. The arrows at the lower end of the cylinders indicate the signaling to the downstream effectors, with plus and minus signs indicating the signaling levels relative to the basal state.

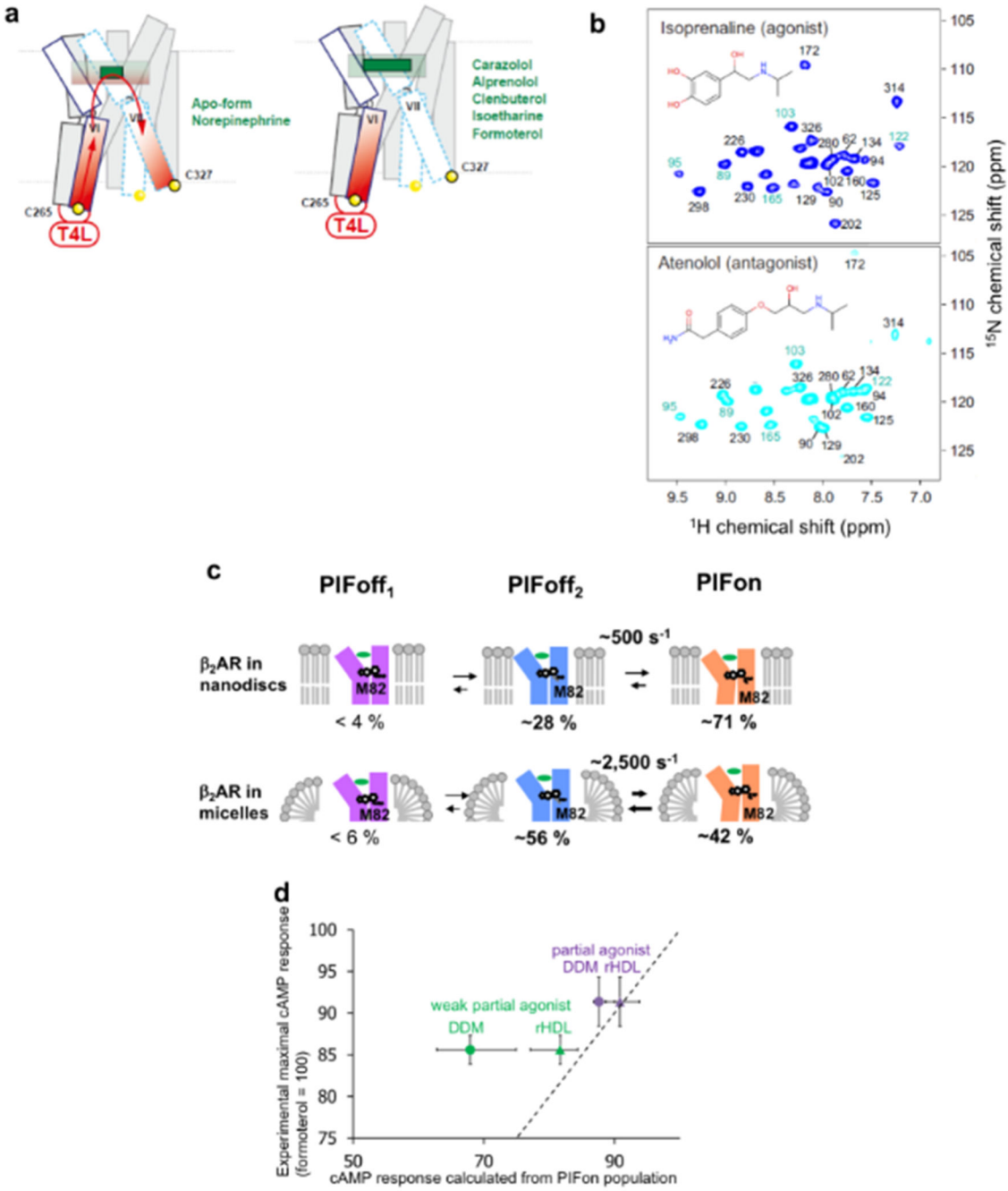

Figure 5 |. Effects on local conformational equilibria of β-adrenergic receptors from different experimental set-ups.

a | Schematic side view representations of β_2AR-T4L visualizing the effects of T4L-fusion into ICL3 on local conformational equilibria related to the G-protein and arrestin signaling pathways, as observed with ^{19}F-NMR probes at positions 265 and 327[123] (see also Fig. 4). The transmembrane helices TMI to TMV are shaded in gray. TMVII, which is in equilibrium between two conformational states manifested by different NMR chemical shifts of a ^{19}F probe attached to C327, is represented as dashed cyan rectangles. TMVI, which is blocked in an active-like state by the T4L fusion, is represented by solid blue rectangles. The

T4L fusion protein is depicted as a small red oval, the direction of its impact on local conformational equilibria is indicated by red arrows, and increased intensity of its impact is indicated by increased density of the red shading. The positions of the ^{19}F-NMR labels are shown by yellow spheres, where the active-like state is further identified by a black circle. The orthosteric ligand binding cavity is indicated by shading. The left panel represents the ligand-binding cavity in the complex with the small ligand norepinephrine (small green rectangle; in the apo-form the cavity does not contain a ligand); the red arrows indicate that a long-range effect from T4L via the orthosteric ligand binding cavity causes a shift in the conformational equilibrium at the intracellular tip of TMVII. The right panel shows the orthosteric binding site containing one of the listed larger ligands (green rectangle); the long-range effect from T4L to TMVII is suppressed by the presence of these ligands, which carry a hydrophobic substituent at the ethanolamine end. **b** | [^{15}N,^{1}H]-TROSY correlation NMR spectra of thermostabilized turkey β_1AR (TS-β_1AR) containing selective ^{15}N-labeling of its 28 valines in antagonist-bound and agonist-bound states. Resonances are marked with assignment information (black, firm; cyan, tentative). The ligand chemical structures are shown as inserts. **c** | Differences between corresponding exchange rates and populations of conformational substates in β_2AR in nanodiscs and in DDM micelles[121]. The upper and lower panels visualize conformational equilibria of the β_2AR complex with the weak partial agonist tulobuterol in nanodiscs and in DDM micelles, respectively. Approximate relative populations of the three states are indicated below the drawings. **d** | Correlation between the simulated cAMP response based on the PIFon populations observed in the M82 NMR signal and the experimental maximal cAMP responses. Plots of the relative amounts, in percent, of cAMP formed upon activation of CHO-K1 cells by the partial agonists tulobuterol and clenbuterol, which were previously identified as such by cAMP accumulation assays[121], *versus* the relative concentration of cAMP in activated cells calculated from the measured populations of PIFon. Both values were normalized to those in the fully active states, and thus are expected to be close to each other whenever the PIFon populations determined by NMR were similar to those *in vivo*. Circles and triangles represent the cAMP responses based on the PIFon populations of β_2AR in DDM micelles and in nanodiscs, respectively. The dotted line represents the hypothetical situation where the simulated cAMP response would be equal to the experimental maximal cAMP response. The error bars along the horizontal axis represent the cAMP concentrations calculated based on the lowest and highest PIFon populations estimated from the M82 NMR signals.

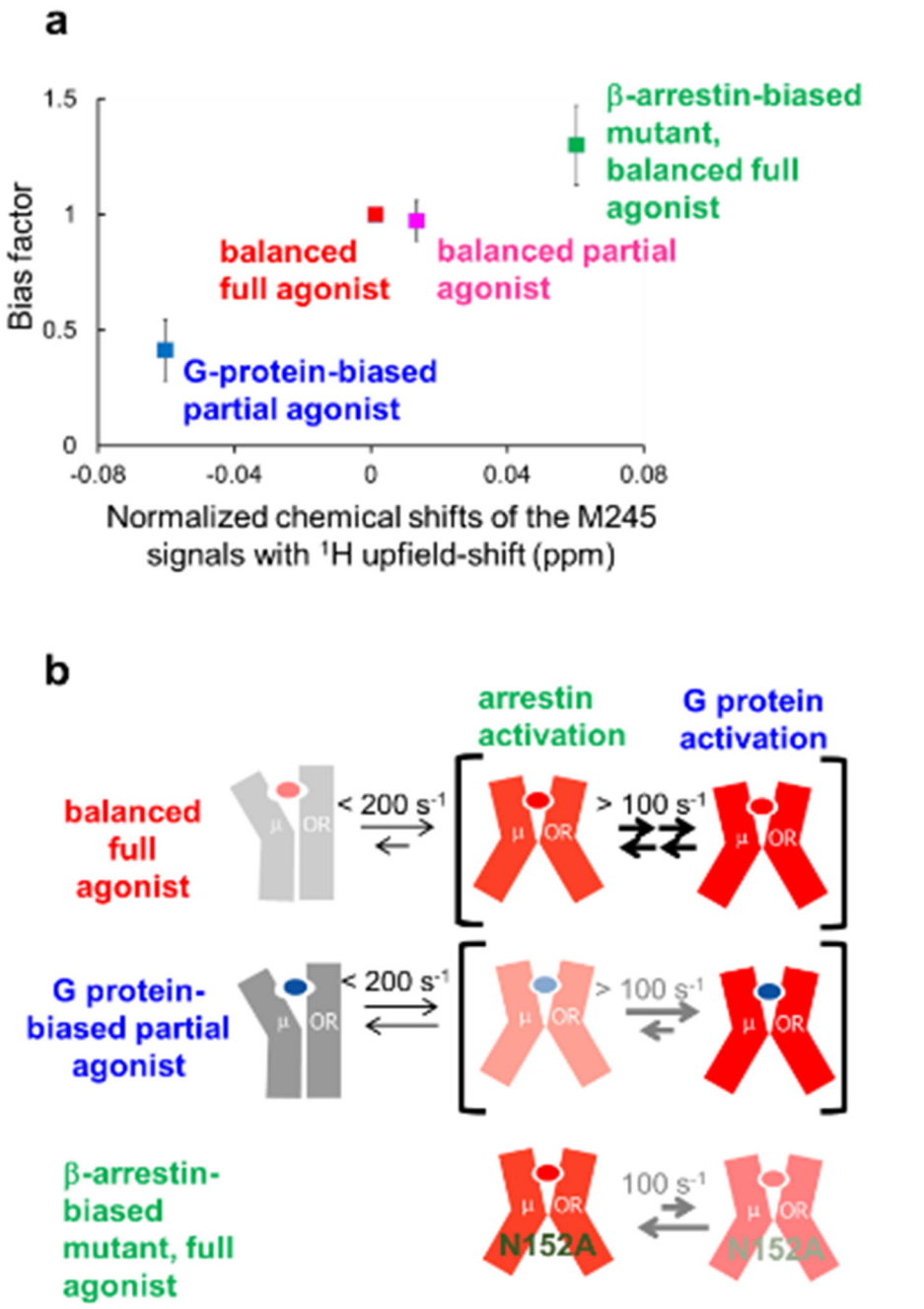

Figure 6 |. NMR-observable conformational equilibria related to biased signaling of MOR.
a | Correlation between the normalized chemical shifts of the M245 NMR signals and the value of the bias factor, which is the ratio of the β-arrestin signaling efficacy to the G protein signaling efficacy. **b** | Mechanisms leading to functional selectivity of MOR for different ligands. In the balanced full agonist state with DAMGO bound, MOR primarily adopts the active conformation (red), in which the intracellular surface is characterized by multiple substates, with exchange rates larger than 100 s^{-1}. In the G protein-biased partial agonist TRV130-bound state, MOR exists in an equilibrium between the inactive (grey) and active

conformations, with exchange rates smaller than 200 s^{-1}, and the equilibrium within the active substates is shifted toward the conformation preferred for G protein activation. In the DAMGO-bound state of the MOR N152$^{3.35}$A mutant, where MOR adopts only the active conformation, the equilibrium among the active substates is shifted toward the conformation preferred for arrestin activation.

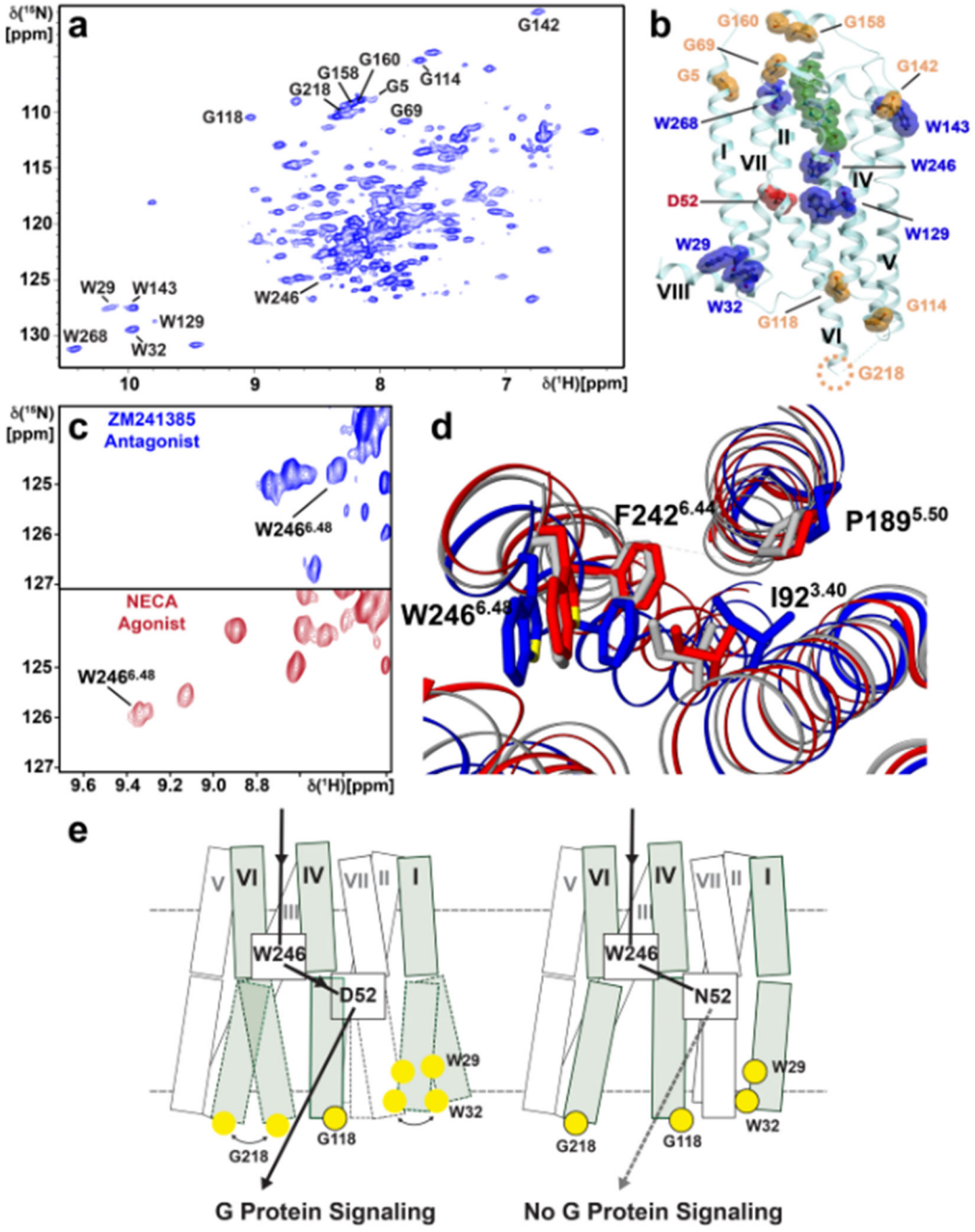

Figure 7. NMR affords a global view of $A_{2A}AR$ response to variable drug efficacy and inactivation of an allosteric center.

a | [^{15}N,^{1}H]-TROSY NMR correlation spectrum of [u-^{15}N, ~70% ^{2}H]-$A_{2A}AR$ in complex with the antagonist ZM241385. Assigned backbone ^{15}N–^{1}H glycine and indole ^{15}N–^{1}H tryptophan signals are annotated. **b** | Locations of assigned glycine (orange) and tryptophan (blue) signals in the crystal structure of $A_{2A}AR$ in complex with the antagonist ZM241385 (PDB 6AQF). ZM241385 is shown in green. D52$^{2.50}$, a critical residue in the allosteric center, is shown in red. Helices are labeled with Roman numerals. The position of G218 is

indicated by a dotted circle, as it was replaced with a fusion protein to facilitate crystallization. **c |** The indole ^{15}N–^{1}H signal of W246$^{6.48}$, the so-called “toggle switch” tryptophan[276,277], is highly responsive to variable drug efficacy, as observed by comparing NMR spectra for $A_{2A}AR$ in complex with the antagonist ZM241385 (blue) and agonist NECA (red). **d |** The response of the W246$^{6.48}$ indole ^{15}N–^{1}H signal to variable drug efficacy can be rationalized by reorientation of the nearby F242$^{6.44}$ in the P/I/F activation motif, which is highly conserved among Class A GPCRs. **e |** Schematic side views of $A_{2A}AR$ (left) and $A_{2A}AR$[D52N] (right). Each transmembrane helix is represented by two adjoining rectangles. The three helices carrying NMR reporter groups near the intracellular surface are shaded, and the residues with assigned NMR lines are indicated by yellow spheres, where black framed spheres indicate that a single NMR line was observed, and unframed spheres correspond to multiple-component signals. The helices drawn with broken lines indicate local polymorphisms seen in the NMR spectra of the residues with unframed yellow spheres. The broken horizontal lines indicate the extracellular and intracellular membrane surfaces. The black arrow indicates the signaling pathway from the orthosteric drug binding site to the intra- cellular surface. In $A_{2A}AR$, signaling has been correlated with local polymorphisms at the intracellular tips of the helices I and VI. In $A_{2A}AR$[D52N], signaling to the intracellular surface is quenched. The broken arrow indicates loss of signaling to the G protein, which correlates with the abolishment of the dynamic polymorphisms at the intracellular surface.

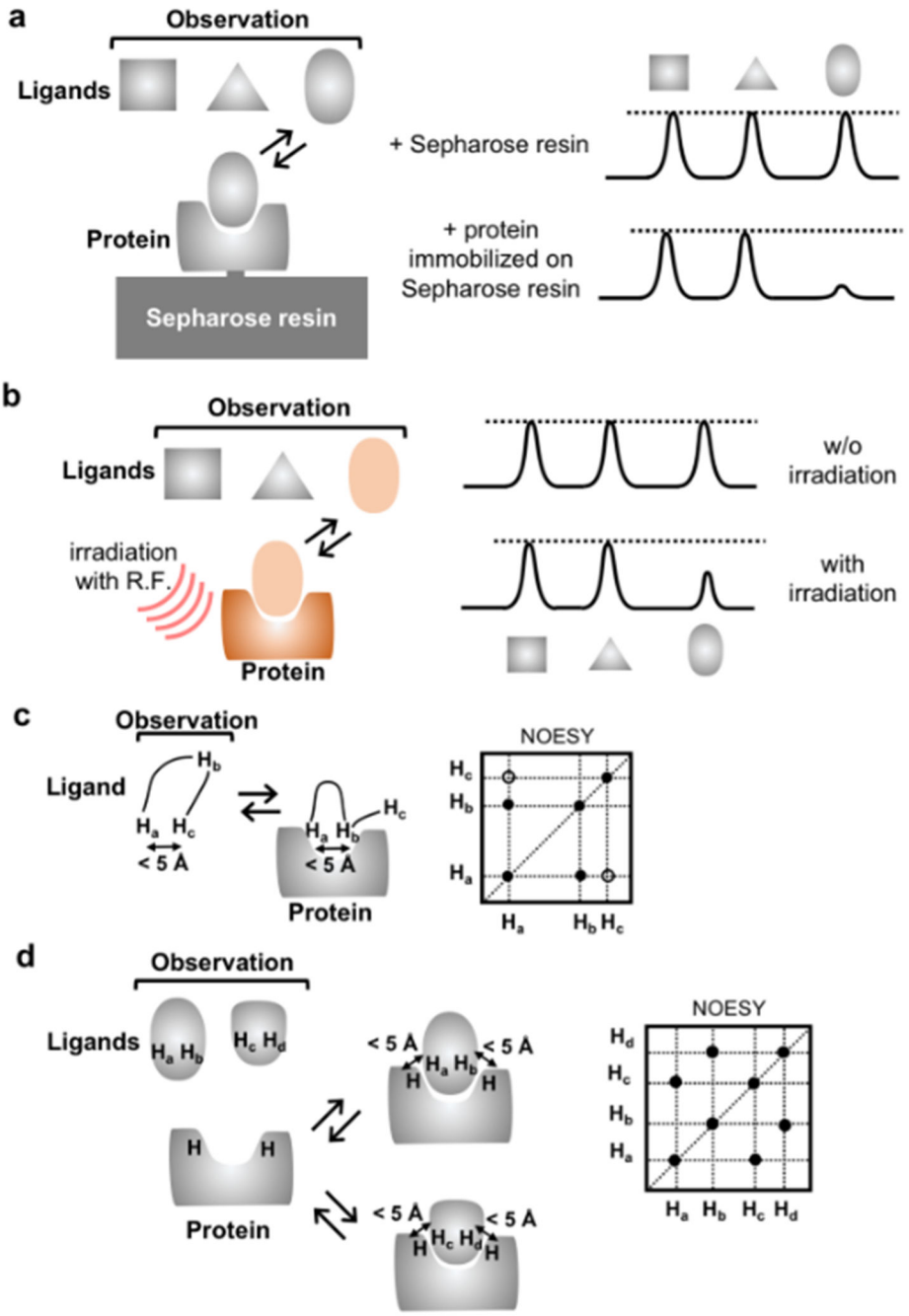

Figure 8. |. NMR methods for studies of GPCR–ligand interactions.

a | Target-immobilized NMR screening (TINS). Resonance broadening of ligands upon binding to proteins immobilized on Sepharose resin is observed. The bound ligand can be identified by the broadening of its ligand signals. **b** | Saturation transfer difference (STD) NMR. The protein–ligand complex is irradiated at a frequency corresponding to hydrogen atoms of the protein, so that saturation can be transferred from the protein to the ligand. If the complex has sufficiently large ligand exchange rates, then this saturation is transferred to the bulk free ligands. The bound ligand can be identified by the transferred saturation. **c** |

Transfer NOE (trNOE). Similar to (b): negative NOEs on the bound ligand are transferred by rapid ligand exchange to the bulk of free ligands. Therefore, trNOEs provide information on distances between protons of the ligand in the receptor-bound state. **d** | Interligand NOEs for pharmacophore mapping (INPHARMA). Protein-mediated NOEs between two or multiple simultaneously bound ligands are observed. Thus, INPHARMA peaks describe the orientation of the two ligands relative to each other in the receptor binding pocket.

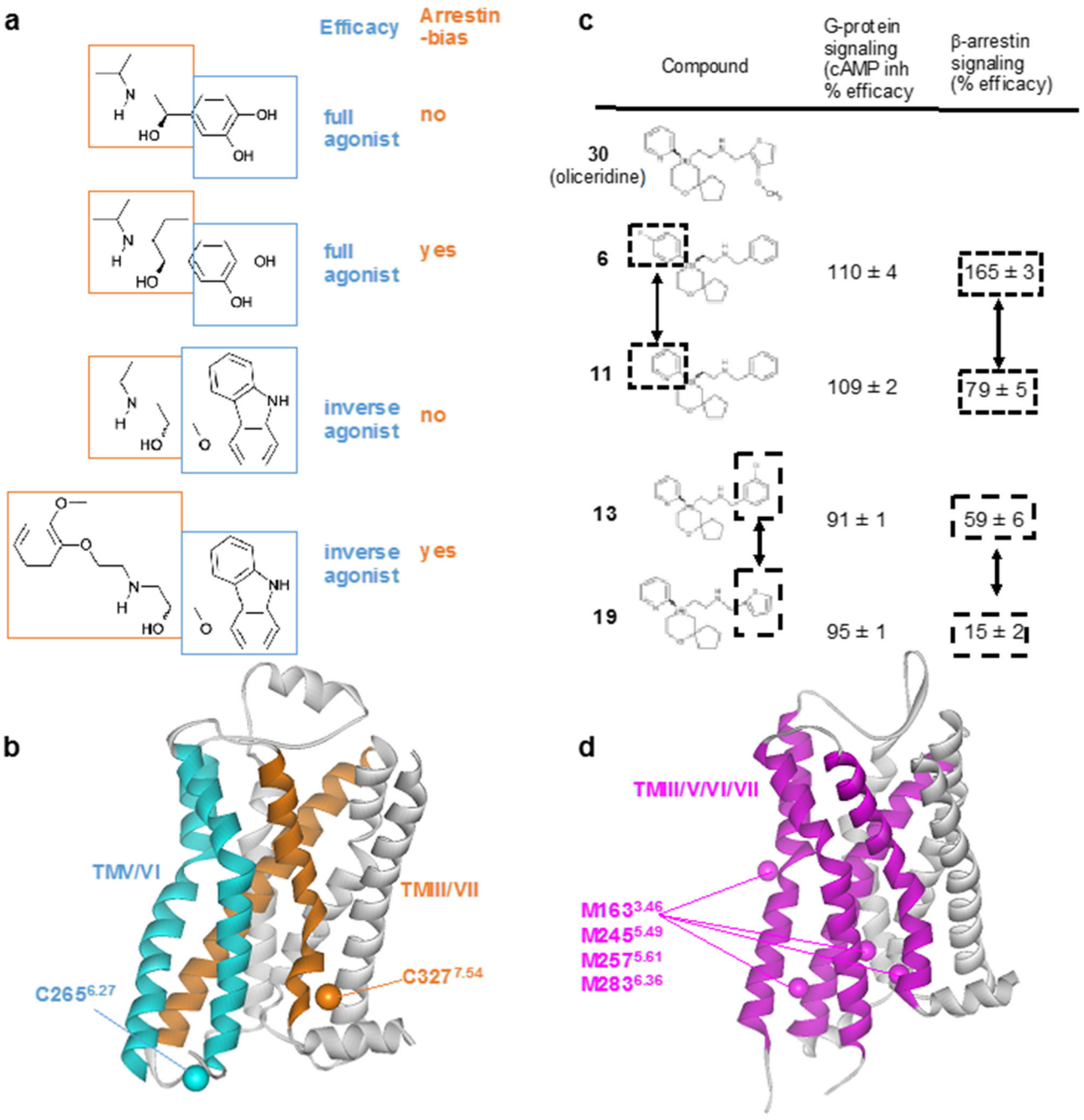

Figure 9 |. NMR screening of biased ligands.

a | Structures and functions of β_2AR ligands. Modifications of the ethanolamine tail moieties (highlighted in orange boxes) result in selective modulation of the efficacies for β-arrestin signaling, whereas modifications of the aromatic head groups (highlighted in blue boxes) affect the efficacies of both G protein-mediated signaling and β-arrestin-mediated signaling. **b** | Crystal structure of the β_2AR complex with the inverse agonist carazolol (PDB: 2RH1). TMV and TMVI (cyan) form the binding site for the aromatic head groups shown in (a). TMIII and TMVII (orange) form the binding site for the ethanolamine tail moieties shown in

(a). ^{19}F-NMR probes introduced at C265$^{6.27}$ (Cβ is shown cyan) enable studies of the roles of TMV and TMVI for G protein signaling efficacy. ^{19}F-NMR probes introduced at C327$^{7.54}$ (Cβ is shown orange) enable studies of TMIII and TMVII in arrestin bias. **c** | Structure–function relationships of derivatives of the MOR ligand oliceridine. Modification of either of the two aromatic rings that are highlighted in boxes results in selective modulation of β-arrestin signaling. **d** | Crystal structure of MOR with a morphinan antagonist (PDB: 4DKL). TMIII, TMV, TMVI and TMVII are shown as purple ribbons, and Cε atoms from M163$^{3.46}$, M245$^{5.49}$, M257$^{5.61}$, M283$^{6.36}$ are shown as purple spheres. NMR studies observing $^{13}CH_3$ groups of these four methionines suggest that TMIII, TMV, TMVI and TMVII are involved in G protein/arrestin signaling bias.

Table 1.

Survey of NMR Studies of GPCRs

GPCR	NMR Labels	Expression System	Membrane Mimetic	ref.
β_2AR	$^{13}CH_3$-Lys	Sf9	DDM	116
β_2AR	^{19}F-TET	Sf9	DDM/CHS	112
β_2AR	$^{13}CH_3$-Met	*expres*SF+	DDM	113
β_2AR	^{19}F-BTFA	Sf9	DDM and LMNG	117
β_2AR	$^{13}CH_3$-Met	Sf9	DDM	118
β_2AR	^{19}F-BTFA	Sf9	LMNG	119
β_2AR	^{19}F-TET	Sf9	DDM/CHS	120
β_2AR	$^{13}CH_3$-Met, ^{2}H	*expres*SF+	nanodisc	121
β_2AR	^{19}F-BTFMA	Sf9	DDM	122
β_2AR-T4L	^{19}F-TET	Sf9	DDM/CHS	123
β_2AR	$^{13}CH_3$-Met, ^{2}H Cterm-^{2}H, ^{13}C, ^{15}N	*expres*SF+ + *E. coli* (segmental label)	nanodisc	124
β_1AR	^{15}N-Val	High Five	DM	114
β_1AR	$^{13}CH_3$-Met	Sf9/Sf21	LMNG	115
BLT2	$^{13}CH_3$-Ile	*E. coli*	nanodisc	130
A_{2A}AR	^{19}F-BTFMA	*P. pastoris*	LMNG/CHS	125
A_{2A}AR	$^{13}CH_3$-Ile, ^{2}H	*P. pastoris*	DDM	126
A_{2A}AR	u-^{15}N, ~70% ^{2}H	*P. pastoris*	LMNG/CHS	127
A_{2A}AR	^{19}F-BTFMA	*P. pastoris*	LMNG/CHS	131
MOR	$^{13}CH_3$-Met, ^{2}H	*expres*SF+	LMNG/CHS	128
MOR	$^{13}CH_3$-Lys	Sf9	LMNG/CHS	129